317001

A REPORT ON

AN EIP AND MIP SURVEY

OVER THE KAPI GRID

NEAR RENISON BELL, WEST COAST TASMANIA

ON BEHALF OF

RENISON LIMITED

E.L. 42/71

JN Jun

J00

317002

PRIVATE AND CONFIDENTIAL

A REPORT ON
AN ELECTRICAL AND MAGNETIC INDUCED POLARIZATION SURVEY
OVER THE KAPI GRID
NEAR RENISON BELL, WEST COAST TASMANIA
ON BEHALF OF
RENISON LIMITED

E.L. 42/71.

BY

A.W. HOWLAND-ROSE
MSc,DIC,AMAusIMM,FGS.
GEOPHYSICIST

SYDNEY, N.S.W.

APRIL, 1977
TAS-037

CONTENTS

SCINTREX PTY. LTD.
GEOPHYSICAL CONSULTANTS AND CONTRACTORS

SUMMARY

The electrical induced polarization gradient array survey carried out over the Kapi Fault grid has, together with the total magnetic field data, enabled an excellent physical property map to be constructed. The strike appears to be grid north-south, with a number of north-east/south-west dislocations being evident.

The position of the Kapi Fault, however, is not readily apparent in spite of the excellent data obtained for all three properties. It is considered that a study of this data in conjunction with the detailed geology available, will assist in a more definitive placement of the Kapi Fault zone.

A number of material induced polarization anomalies were located, each of which is described and interpreted in the text.

1031 WELLINGTON STREET, WEST PERTH, W.A. 6005 TELEPHONE: 21 6934 TELEX: 92353 TELEGRAMS: SCINTREX, PERTH

6 TRAMORE PLACE, KILLARNEY HEIGHTS, N.S.W. 2087 TELEPHONE: 451 5367 TELEX: 26859 TELEGRAMS: SCINTREX, SYDNEY

03

317005

A REPORT ON
AN ELECTRICAL AND MAGNETIC INDUCED POLARIZATION SURVEY
OVER THE KAPI GRID
NEAR RENISON BELL, WEST COAST TASMANIA
ON BEHALF OF
RENISON LIMITED

INTRODUCTION

At the request of Mr. L. Newnham, Chief Geologist for Renison Limited, Scintrex Pty. Ltd. executed gradient array electrical induced polarization reconnaissance surveys, with some magnetic induced polarization detail work, over the Kapi Grid, near Renison Bell, West Coast Tasmania.

The work was undertaken by senior operator Mr. B. Ekstrom assisted by operator Mr. G. Street, BSc., on five single operator days and four double operator days between 6th and 16th February, 1977. 1½ days were lost to bad weather and magnetic storm conditions over that period. Field assistants were provided by Renison Limited with Scintrex providing Mr. L. Jones for half the survey period.

On site geological supervison was undertaken by Mr. K. Wells, Senior Exploration Geologist, while the author provided geophysical supervision, and visited the survey team on 9th February, 1977.

The objective of the survey was to map and delineate rock zones

within the Kapi grid area with electrical and/or magnetic induced polarization methods and use these in conjunction with the total field magnetometer data, provided by Renison Limited, to delineate the position of the Kapi Fault.

METHOD AND EQUIPMENT

For both the electrical and magnetic induced polarization surveys, a 10/15KW generator coupled to a Scintrex 15KW transmitter was the energising source. For the gradient array survey, this allowed current dipoles as great as 2800 metres to be used, which made it possible for larger areas to be surveyed from a single set-up. This not only speeded production but enabled greater uniformity in data. Also in this case, lines from adjacent spreads were duplicated, enabling geophysical trends to be clearly assessed over gradient block boundaries.

The receiver used for both the magnetic and electrical induced polarization survey was the Scintrex IPR-8, which in the case of MIP was coupled to a Scintrex MFM-3 horizontal field magnetometer. (specification sheet appended to this report)

A description of the MIP method is appended to this report, while a brief comment on the gradient array method is made below.

This very simple explanation of the parameters measured in the gradient array, is designed specifically for the geologist in

ELECTRICAL PARAMETERS MEASURED

(A) RESISTIVITY MEASUREMENT

(taken during current 'on' time)

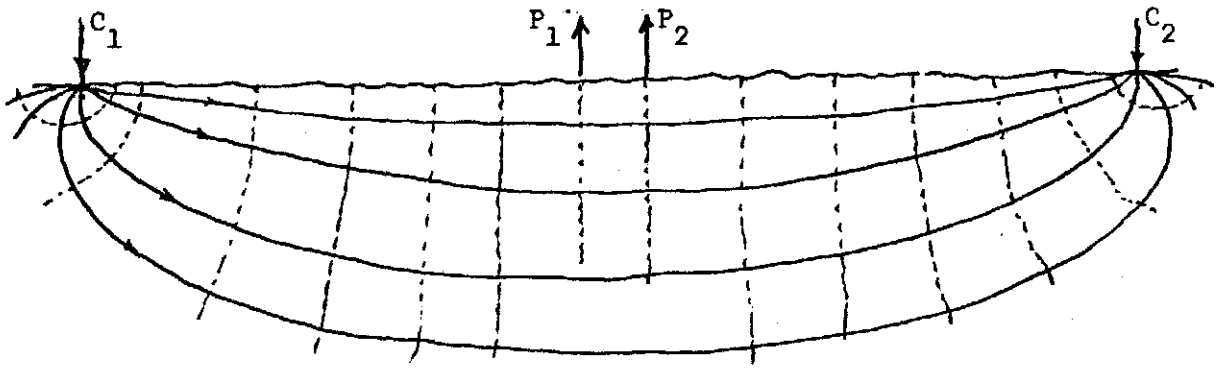

MEASUREMENT REPRESENTS:

ease with which primary current moves through ground

primary current flow
primary equipotential surface

(B) CHARGEABILITY (IP) MEASUREMENT

(taken during current 'off' time)

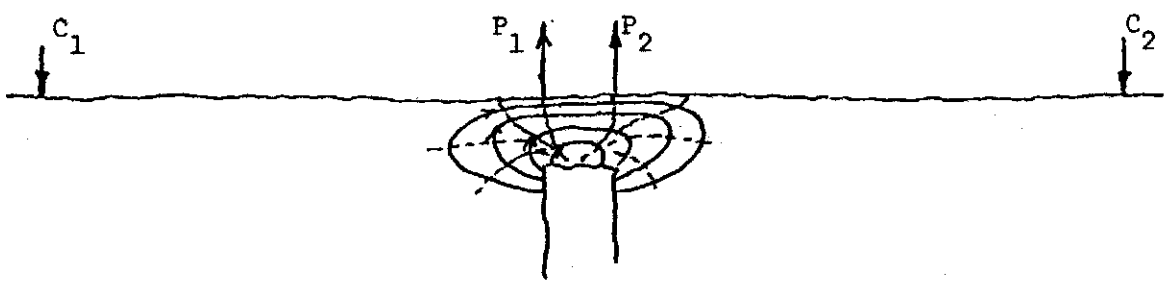

MEASUREMENT REPRESENTS:

discharge of stored energy

secondary current flow
secondary equipotential surface

5 cm

FIGURE 1

order to give a *visual picture* of the parameters measured.

In the case of gradient array, the potential dipole records the electrical properties of the material defined by the two equipotential *surfaces* tapped by the potential electrodes. This is diagramatically illustrated in Figure 1(A). This diagram represents a *section*, however, it should be realised that the apparent resistivity measurements also record information *sideways*. For a three dimensional picture of the volume sampled, rotate the section *into* and *out of* the plane of the paper by 90°. Within the centre section of the array, the data represents the characteristics of the rock units *immediately below* and *immediately at right angles* to the survey line. The degree of *resolution* depends on the potential *dipole width*, the smaller the dipole the greater the resolution. Figure 2 (the resistivity data) demonstrates the much improved resolution for a 10 metre dipole over that obtained from a 25 metre dipole over a sulphide occurrence. It is important to remember when examining the data that only the *gross* properties are "seen". The potential dipole cannot resolve units whose effective width is less than half the size of that dipole.

The criteria affecting the chargeability reading are somewhat different. In Figure 1(B) the decay of a chargeable section is shown. The passage of current during the *current-on* phase, during which the resistivity measurement was taken, carried some energy to be stored in the rocks (and sulphides, etc.), through

IMPORTANCE OF RESOLUTION

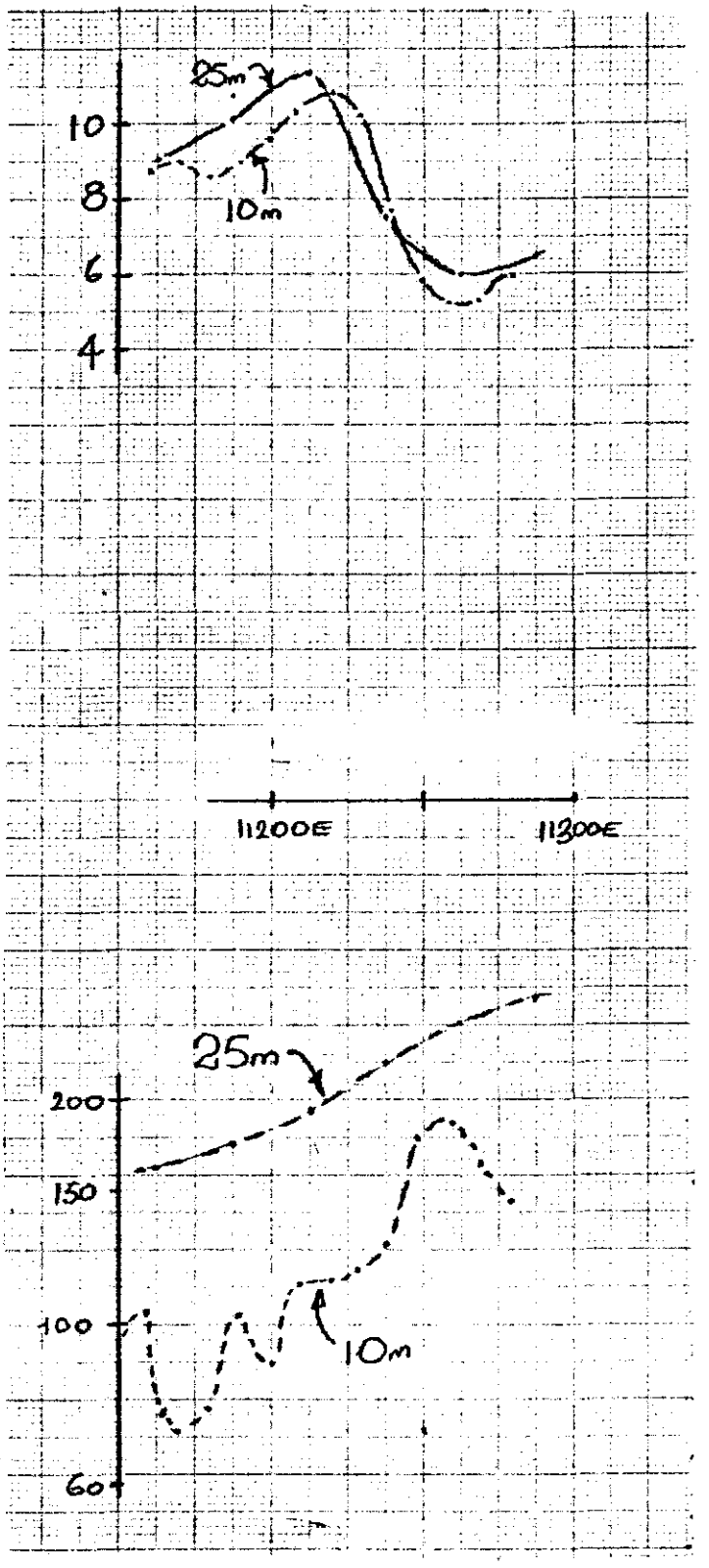

FIGURE 2

5 cm

which it passed. On cessation of this imposed current flow, the energy so stored will discharge (IP). It will set up its own equipotential field as shown in Figure 1(B) which will be detected by the same two potentials which measured the resistivity. It should be noted that any chargeable source will have a width *greater than* the source due to the curvilinear nature of the discharge of the stored energy. It should be further noted that the volume defined by the *secondary potential field* caused by this discharge *is not necessarily identical* to that defined by the primary equipotential field. Figure 2 shows the differences in resolution *for chargeability* (top profile) over a known sulphide occurrence. The *form* is similar, but the positional information is far superior due to the more frequent reading interval.

This array has operational attributes which result in rapid coverage and excellent positional information. However, depth information is not well defined, it being possible only to assess "maximum depths".

With regard to the interpretation of the gradient array data, the following comments may prove to be of assistance.

In the gradient array the source of the reading lies between the two equipotential surfaces tapped by the two potential pots employed. For the most part then, when working in the centre section of a gradient array, the source will be "immediately below"

the potential dipole used. The reliability therefore of *positional information* with gradient array is excellent, however, the depth at which the response occurs is difficult to assess with accuracy. The *maximum depth* can be estimated from a consideration of the profile shape, but the accuracy of this approach will depend on a minimal potential dipole length, and of course sharp boundaries to the body. The *resolution* therefore is not better than half of that dipole. Therefore maximum depths of 10 metres may in fact either outcrop or sub-outcrop when a 20 metre potential dipole is used. Some moving source array would be required to obtain an *accurate depth estimate*.

Similarly the width of bodies is not easy to determine for zones having a width less than half the dipole spacings used. Thus, estimated maximum widths are educated guesses at best for narrow zones. However, wider bodies can be resolved more accurately.

The *attitude* of a chargeable zone can really only be gauged with any precision in the centre of the gradient array, and of course where the body has strongly contrasting chargeability and apparent resistivity to that of the enclosing rock units.

All field measurements were taken between slope distances along lines. This will, in steep areas, produce errors in the calculated apparent resistivity data. However, these errors will be arithmetic, and as significant changes in resistivity are logarithmic, this

source of error is not significant. In assessing the position of the source in areas of extreme terrain, it does not lie vertically below the plotted position, but *normal to the "local slope"*. All positions in the text refer to source positions normal to the local slope.

Each current dipole block should be considered separately. As would be expected, the continuity along strike is generally good, especially in the chargeability data. Although not applicable in this case, *"end-on"* current dipole blocks cannot be expected to give identical data due to the different base levels of the current dipoles, and in zones close to the current poles, the data will not sample identical volumes on the overlap between current dipoles. This phenomenon will result in more extreme divergence of data as the current dipole is approached. However, these factors are entirely predictable.

THE MIP PARAMETERS

The parameters used for the display of the MIP data require some explanation in order that you will be able to put a physical meaning to them in your evaluation of the data.

H_N This parameter is termed the *normalised horizontal magnetic field* and is expressed as a percent of *normal*. This quantity represents the ease with which the energising current flows through the ground between the two energising electrodes, which

were placed parallel to strike. For example, if the ground were everywhere homogeneously resistive (or conductive) the H_N would be 100%. Where H_N is higher the ground is more conductive, and where it is lower, it is more resistive. You can regard this parameter as *"relative conductivity"* plotted upwards.

H_S This parameter is known as the *secondary magnetic field*, and is the *actual* magnetic field associated with the current flow in the ground caused by the discharge of the stored *induced polarization* energy in the sulphide source.

M & ΔM This is analagous to the EIP chargeability but is expressed as *milligamma/gamma*. Now, as the magnetic sensor is able to sense the *form* of the decay *inside* the source, we can differentiate mineral assemblages which have markedly different characteristics such as *grain size* of mineral types (e.g. graphite versus magnetite versus sulphides).

Very briefly, fine grained mineralisation absorbs the charge *rapidly* and once the passage of the energising current is stopped, the stored charge is *rapidly* discharged. If the mineralisation is *effectively* coarse grained (i.e. either coarse grained as such or agglomerates of finer grain) the charging and consequent discharging will be be much *slower*. Only with MIP is the actual decay within the source monitored, therefore major differences in decay characteristics can be observed. Diagram 1 shows how

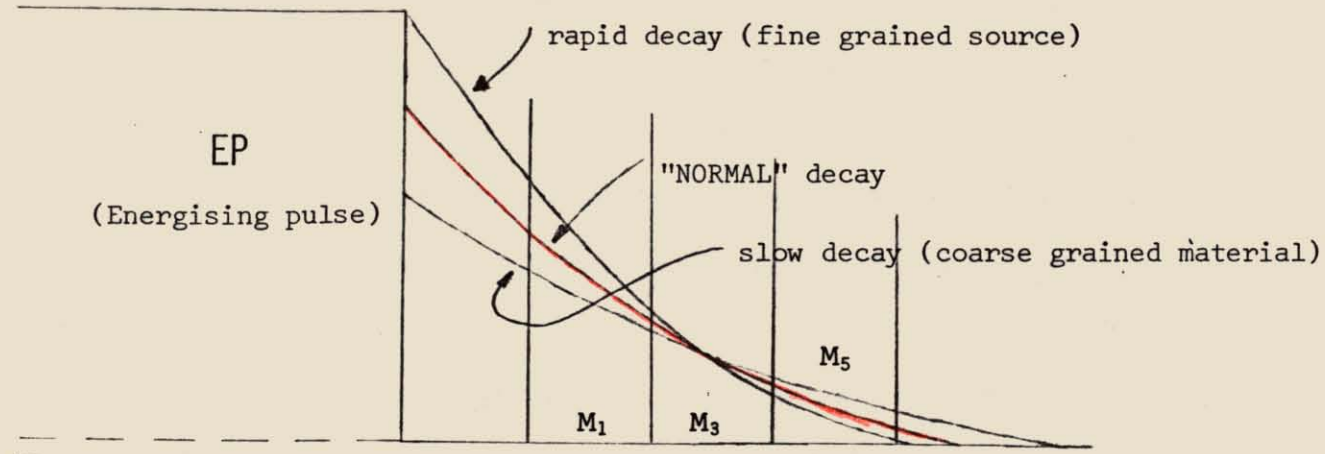

(A) DECAY AS OBSERVED BY IPR-8 MIP RECEIVER PRIOR TO PROCESSING

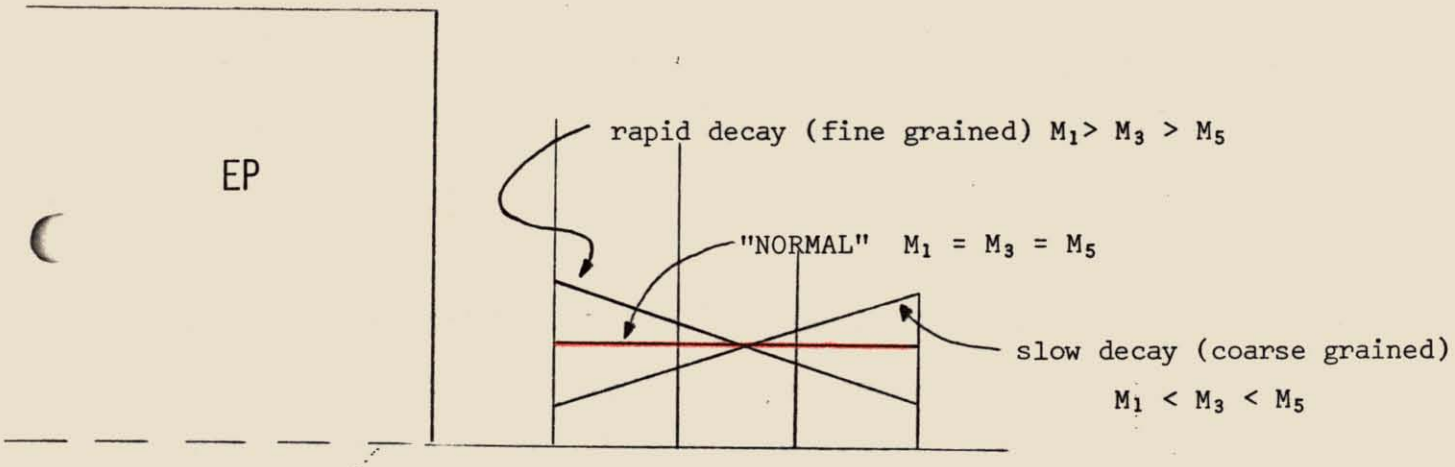

(B) DECAY AS OBSERVED BY IPR-8 MIP RECEIVER AFTER NORMALISATION FOR A "NORMAL" DECAY FORM

DIAGRAM 1

this is accomplished using the IPR-8 time domain receiver. In sketch (A) EP represents the energising pulse, while the rapid decay form is due to fine grained material discharge, and the slow decay form is due to coarse grained mineralisation. You will note from the diagram that the rapid decay form has a greater amplitude to start with. This is due to the fact that as the IP effect depends on the total surface area of the sulphides presented, the disseminated material per sulphide volume present will give a greater IP effect.

All three slices were recorded. These three slices are shown in the diagram as M_1, M_3, and M_5. The red decay form included in Diagram 1(B) is the 'normal' or 'average' decay form usually observed over normal rocks. The IPR-8 processes the data by dividing this normal decay into each of the slices M_1, M_3 and M_5. This is done so that any deviation from "normal" is readily apparent. Diagram 1(B) displays the result of this processing of data. The rapid decay form (e.g. fine grained disseminated) will result in $M_1 > M_3 > M_5$, while the slow decay form (e.g. coarse grained massive, but not necessarily electrically continuous) will result in $M_1 < M_3 < M_5$.

The ΔM parameter plotted on the chargeability profiles is a short hand display of the decay form; ΔM being equal to $|M_5| - |M_1|$. Thus, when this quantity is *positive* it infers *coarse* grain size, and when *negative* infers *fine* grain size for a given mineral.

DATA PRESENTATION

As instructed, the chargeability and apparent resistivity data was drafted onto Renison standard 1:5000 sheets. However, photocopies of the corrected EIP field data profiles at the scale of 1:2500 have also been presented with this report. The MIP data profiles are appended to this report at the horizontal scale of 1:2500 and vertical scales as follows:

Chargeability, M_1, M_3 and M_5	1 centimetre = 1 milligamma/gamma
Decay Rate, ΔM	1 centimetre = 1 milligamma/gamma
Normalised Horizontal Magnetic Field, H_N	1 centimetre = 10%
Secondary Magnetic Field, H_S	1 centimetre = 1 milligamma/ampere

The apparent chargeability, apparent resistivity and total magnetic field data have been contoured at the scale of 1:5000 and are presented on Plates 2, 3 and 4 respectively.

Plate 5, also at the scale of 1:5000, contains a "Summary of the Geophysical Characteristics" as observed on Plates 2, 3 and 4, while Plate 6 is an interpretation plan at the same scale. It should be noted that the existing known geology *has not* been used in the construction of these geophysical contour plans or interpretation.

DISCUSSION OF RESULTS

The contour presentations are discussed first then the composite interpretation maps, and finally the salient features of the data profiles.

The Apparent Chargeability Contour Plan (Plate 2)

The apparent strike over the entire grid varies *about* grid north-south, with material variations along the grid. Between 100N and 1500N, rarely are chargeabilities below 35 millivolts/volt, with individual maxima rising to 50 to 70 millivolts/volt. Between 1500N and 2300N, the background chargeability decreases rapidly to about 10 millivolts/volt with anomalies rising to 30 millivolts/volt in the eastern and central sections. Again, the strike is clearly grid north-south. Between 2300N and 2900N, apparent chargeabilities are an abnormal 7 $\pm$4 millivolts/volt, again with an apparent grid north-south trend. On line 15900N, apparent chargeabilities increase dramatically to over 100 millivolts/volt, but their trend cannot be clearly established.

The Apparent Resistivity Contour Plan (Plate 3)

The grid area has been divided into four distinct units by three grid north-east/south-west trending "diclocations". It is not known whether these "dislocations" are "flexures" or "faults", but they are seen dramatically on both the magnetic and apparent resistivity data, although not so prominently on the apparent chargeability data. (For their approximate locations, see Plates

5 and 6)

D1 crosses line 300N at about 650W onto line 1100N at 100E(projected). To the south, resistivities are a high 1000 ohm-metres east of 100N/500W - 300N/475W. East of this boundary, background chargeabilities are 35 millivolts/volt. This is considered to be a distinct geological unit.

To the north of the above boundary, the resistivity falls to 300 to 500 ohm-metres, but the chargeability rises to 50 ±5 millivolts/volt. This unit is also considered a distinct geological unit.

Both the above zones have been mapped as Upper Cambrian Conglomerate and grits (€uc). The apparent resistivities would fit this description, but the high chargeabilities indicate a high mafic mineral content and/or anomalously high graphite or sulphide content. Magnetite content is however, low, as the magnetic field is relatively uneventful.

Between dislocations D1 and D2 which crosses 1500N/700W (projected) and 1900N/150W, the characteristics are quite different. To the west, higher apparent resistivities in excess of 1000 ohm-metres (e.g. 1300N/450W) to as little as 15 ohm-metres 125 metres to the east were recorded. This distinct low *may* mark the position of the Kapi Fault zone. Further to the east, apparent resistivities

increase again to over 1500 ohm-metres. This sequence could represent individual rock types whose approximate strike is grid north-south, and as the mapped rocks in the area are Upper Cambrian shales, tuffs, schist and siltstones (€us), certainly the variations in apparent resistivity could well be explained by variation in rock types.

The resistivity lows *could* be due to more conductive shales and/or tuffs, while the more resistive units such as siltstones *could* be shown up by the more resistive units.

In the easternmost section surveyed, the higher resistivities of 1000 to 1500 ohm-metres coincide with higher chargeabilities of 45 ±5 millivolts/volt. These characteristics are very similar to those seen to the south of D1, namely the Upper Cambrian Conglomerates and grit unit (€uc).

To the north of dislocation D2 up to dislocation D3, which makes a shallow angle with line 2700N crossing it at *about* 400W, apparent resistivities fall dramatically. On the westernmost section surveyed, resistivities are a high 1000+ ohm-metres, reaching 3000 ohm-metres on line 2100N, but rapidly fall to less than 300 at 250W on the same line, and to 50 ohm-metres at about 150W. Further to the east, resistivities rise again to 300 ohm-metres. Now this sequence is very similar to that seen between D1/D2 to the south. The *clear impression* is that this entire block is

shifted east by folding and/or faulting along D2. The extreme changes seen in the apparent resistivity could again be due to the variations in geophysical characteristics below the resistive siltstones and more conductive tuffs/shales (?)

A further dislocation D3 is suggested which crosses lines 2500N and 2700N at *about* 700W and 400W. This is not so clearly seen on the apparent resistivity data, however, the total field magnetic contour plan clearly *confirms* its presence.

To the east of about 2900N/140W and 15900N/350W, higher resistivities of up to 1500 ohm-metres, in association with higher chargeabilities of 30 to 35 millivolts/volt were recorded. These characteristics are similar to those recorded over the Upper Cambrian Conglomerates and grits (€uc) in the far southern section of the area. However, the geological map shows Middle Cambrian Ultrabasics (€um) in this area.

Now, the total field magnetometer survey shows a real variation in characteristics, with the magnetic field showing activity of over 500 gamma above the local base. The strike appears to be grid north-south. The additional dimension of the magnetic field data for differentiating units which otherwise have the same geophysical characteristics is well demonstrated in this case.

To the west of the above boundary, resistivities again fall

dramatically to below 150 ohm-metres, while the magnetic field becomes more subdued on line 2900N. On line 15900N resistivities *fall* but chargeabilities *rise*. This infers different rock types underlie each of these lines (see Plate 6).

The Magnetic Field Contour Plan (Plate 4)

The "base level" for the field in the area is between 62,600 gamma in the southern section of the surveyed grid to about 62,000 gamma in the northern section.

Dislocations D2 and D3 are clearly seen on the magnetic contour map, however, the dislocation D1 is really not observed at all. This is due to D1 occurring wholly within sedimentary rock units of uniform magnetic level.

The strike direction clearly inferred by the magnetic data is grid north-south between dislocations D2 and D3, and beyond.

The most prominent feature noted in the magnetic field was a relatively "narrow ridge" which rises some 1200 to 1600 gamma above background on lines 1900N, 2100N, 2300N and 2500N at about 340W, 270W, 290W and 300W respectively. At either end it is sharply truncated by dislocations D2 and D3. Now this distinct feature is associated with a sharp change in apparent resistivity from over 1500 ohm-metres to the west to as little as 50 ohm-metres to the east. The magnetic high itself, however, is about 150

to 300 ohm-metres. The chargeability data shows some of the lowest values over this zone, as low as 5 millivolts/volt over the northern half. In summary then, this feature marks a *change* in rock type, lies within anomalously low chargeabilities, and is itself 1000+ gamma above background. It could represent a unique rock type, such as an ultrabasic intrusive, for *some* serpentinites show anomalously *low* chargeability, but it may also mark a magnetite bearing intrusive *along* the Kapi Fault. So it is possible it follows either the *resistivity low* or the *change in resistivity* which is coincident with this narrow (intrusive?) magnetic high.

Now to the south of D2, several isolated magnetic highs of the same order as the "magnetic ridge" (i.e. 1000 to 1500 gamma) occur, e.g. 1700N/175W and 1100N/100W. These units do not appear to materially influence the apparent resistivity data, so presumably they are either of resistivities close to those around them, or of too small dimensions to influence the nett apparent resistivity observed. The northernmost of these small magnetic highs is contiguous to a marked apparent chargeability low of smaller order than that associated with the "magnetic ridge", while the southern magnetic high does not influence the data materially. Now, as both occur close to mapped contacts (see preliminary geological map) both *may* represent small, narrow intrusives of magnetite with ultramafic (such as serpentine) minerals.

To the north of the dislocation, D3, the western section of lines

2900N and 15900N are seen to be more magnetically active, with local highs of up to 300 gamma above the background. As this coincides with higher resistivities, this confirms the presence of basic to ultrabasic units mapped in the area. Some sections show higher chargeabilities (to the east) while others show low chargeability (to the west). Thus there are two types of ultra-basic present.

The extreme western section of line 15900N represents quite a distinct sequence with high magnetic field, high chargeability and low resistivities typical of serpentinites.

Summary of Geophysical Properties (Plate 5)

Plate 5 emphasises the *strike direction* and *extent* of the significant geophysical features and suggests three zones of dislocation, D1, D2 and D3, all of which trend grid north-east to south-west. As each of these features has been described in detail above, no further explanation is given here as Plate 5 is in fact a summary of the above discussion.

Interpretation Plan (Plate 6)

This plan is an interpretation of the geophysical data into a function of the geology which lies beneath. The extent of each of the physical property units is shown, together with variations within them. Each is coded as follows..

Resistivity	Chargeability	Magnetics
R = resistive	C = chargeable	M = high
) = conductive	¢ = non-chargeable	B = background
O = intermediate	O = intermediate	

Thus RCM indicates the unit to be resistive (R) chargeable (C) and magnetic (M). Any item underlined infers extreme conditions i.e. R indicates the unit to be extremely resistive.

As can be clearly seen from the contoured data for all three properties, there is a great deal of variation in the amplitude of these properties and, in general, clear-cut boundaries between them. It is also clear that the strike in the area varies about grid north-south, and that the major dislocations, whether they be faults or folds, are grid north-east/south-west. However, fixing the position of the Kapi Fault zone precisely is not easy in spite of all the available detail.

Two possible positions are suggested...

A.....The first is based on the assumption that the fault will be more subject to weathering. In this case it would be expected to follow the low. This suggestion is shown in blue on Plate 6.

B.....That in the case of the zone between D2 and D3 the fault will be marked by a *sharp change* in resistivity, and may in part be marked by the presence of a magnetite rich intrusive. This is

shown in orange on Plate 6.

South of the dislocation D2, the suggested route for the Kapi Fault is along the resistivity low.

The author considers that after a detailed study of the geophysical data contained in this report, together with the available geology the fault will be able to be positioned with much more precision, as the mode of occurrence of the various rock units and their general structural pattern is not really known or understood by the author.

Comments on Individual Lines

Lines 100N and 300N are very similar in form and clearly indicate a grid north-south strike.

The major induced polarization response was observed centred at 662W where slightly higher apparent resistivities of 600 ohm-metres were recorded as against 250 ohm-metres to the west and 375 ohm-metres to the east. A very similar anomaly was centred at 562W on line 300N again with higher resistivities, but with a small *decrease* in apparent resistivity (see profile). The maximum depth to the chargeable source is about 65 to 75 metres. In both cases the anomaly is about 30 millivolts/volt above background. Disseminated sulphides and/or graphitic material within a resistive host is considered to be the source.

Line 500N is in general very similar in form to 300N, however, the higher chargeabilities seen to the west of 512W on 300N are now seen to the west of about 290W on this line. Individual chargeable sources at 388W and 462W of over 10 millivolts/volt above the 45 millivolts/volt background are considered to have disseminated sources at depths no greater than 25 to 30 metres.

On line 700N the apparent resistivity shows a general increase from west to east as seen on all lines to the south, however, the chargeability data shows a distinct change in form. A distinct chargeability anomaly of 8 millivolts/volt between 388W and 437W was associated with higher apparent resistivities. The maximum depth to the essentially disseminated source is considered to be of the order of 40 metres.

A second substantial peak of 14 millivolts/volt above the 42 millivolts/volt background was noted at 262W from within unchanged resistivities of 600 ohm-metres. The disseminated source is considered to have a *maximum* depth of 75 metres, and is probably considerably less than this figure.

The least significant anomaly was about 10 millivolts/volt above the 42 millivolts/volt background, again associated with no change in the 1000 ohm-metres apparent resistivity. The maximum depth to the disseminated source is considered to be about 50 metres.

Line 900N was overlapped from two adjacent set-ups and the data is remarkably alike. Some four distinct induced polarization maxima were observed at 388W of 72 millivolts/volt, at 288W of 40 millivolts/volt, at 162W of 37 millivolts/volt and at 062W of 32 millivolts/volt. All are better than 8 to 10 millivolts/volt against the declining west to east background. The maximum depth to source in each case is about 40 to 50 metres. In the case of the most substantial response of about 72 millivolts/volt at 388W, it is associated with a 90% fall in apparent resistivity to about 70 ohm-metres. Thus, either the source is conductive as such, or the sulphides (or graphite) within it must, in part, be in electrical continuity.

The general *form* of resistivity on line 1100N is similar to 900N. Substantial induced polarization of 20 millivolts/volt above the 30 millivolts/volt background at 337W is associated with a dramatic decline in apparent resistivity from over 600 ohm-metres to east and west to about 20 ohm-metres. The source is very clearly graphite or sulphide in electrical continuity at this point.

A substantial induced polarization anomaly of the same order (30 millivolts/volt above background), was observed between 237W and the response described immediately above. The relatively high 400 ohm-metres apparent resistivity indicates a disseminated graphite or sulphide source at a maximum depth of 10 metres.

The most eastern response observed was of 25 millivolts/volt superimposed on a 22 millivolts/volt background centred at 062W. As there is no material change in the 400 to 500 ohm-metre resistivity, the source is considered to be disseminated in nature. The maximum depth was judged to be about 25 metres.

The resistivity data on line 1300N is very similar to that seen on line 1100N. High background chargeabilities were noted between 150W and the end of the line at about 470W, and within this section, a local maxima of 12 to 14 millivolts/volt was noted at 362W which is coincident with a massive decrease in apparent resistivity from over 1000 ohm-metres to the east and west to less than 10 ohm-metres at 325W. This reponse is from chargeable material, either sulphides or graphite, in electrical continuity (i.e. "massive"). The maximum depth to source is about 25 to 30 metres.

A substantial 40 millivolts/volt above background response was observed centred at 237W from an essentially disseminated source. The maximum depth to source is considered to be 40 metres.

A narrow chargeable zone associated with higher resistivities was noted at 162W. The interpreted disseminated source within a resistive host is about 25 metres below surface.

The main feature on line 1500N is relatively low resistivity of 100 ohm-metres (as against 400 to 500 ohm-metres to the east

and west), between 412W and 288W, coincident with a fall in apparent chargeability of 40 millivolts/volt or so to 8 millivolts/volt. This low *may* represent the site of the Kapi Fault zone.

The high apparent chargeability of about 40 millivolts/volt (10 millivolts/volt above background) centred at 450W is probably associated with the sulphides within the old mine workings. If so, the anomaly recorded at 337W on line 1300N must be of interest.

A substantial 12 millivolts/volt maximum centred at 037W associated with high resistivities of 1000 to 2000 ohm-metres, is due to disseminated sulphides or/and graphite at a maximum depth of the order of 25 to 30 metres.

On line 1700N resistivities and chargeabilities show a fall between 300W and 362W which is considered to correlate with the more pronounced feature centred at 337W on the previously described line (1500N). As with 1500N, chargeabilities rise to the east and west. To the west a peak of 33 millivolts/volt, 8 millivolts/volt above the 25 millivolts/volt background *may* be related to the chargeability from within the mine workings.

To the east, three related chargeability responses at 188W, 237W and 275W of 10 to 16 millivolts/volt above the 20 millivolts/volt

background arise from within apparent resistivities of 150 ohm-metres to 500 ohm-metres. The disseminated sulphides or graphite sources are considered to be no deeper than 25 metres.

East of 150W the apparent chargeability background increases from 25 millivolts/volt to 45 millivolts/volt, with two peaks of 58.5 millivolts/volt and 54.5 millivolts/volt being noted at 140W and 037W, originating in source material of 1000 ohm-metres. The disseminated sources are considered to have maximum depths of 25 and 40 metres respectively.

The main feature seen on line 1900N was lower apparent resistivity between 100W and 350W which rise to the east and west. A dramatic change in induced polarization level from 10-20 millivolts/volt background to the west of 150W to in excess of 45 millivolts/volt at 125W was noted. This is similar to the previous line.

MIP on Line 1900N... A short section of line 1900N was re-run using MIP between 400W and 250W. This data showed a significant 6 milligamma/gamma internal response situated at or east of 262W, accompanied by an increase in H_N. The maximum depth to source is indicated as 75 metres. The host to the mineralisation is conductive.

On line 2100N the same general resistivity low was noted between 100W and 250W (only lower on this line). A distinct chargeability

maximum of 25 millivolts/volt was noted at 040W within 200 ohm-metre resistivities. The essentially disseminated sulphide or graphite source is considered to lie at a maximum depth no greater than 50 metres.

An 18 millivolts/volt anomaly on the 8 millivolts/volt background was defined at 237W. This response occurs on a changing resistivity level, but does not influence it. The source is considered again to be disseminated, and at a maximum depth of 25 metres.

Increased apparent resistivities to over 1000 ohm-metres at 362W are accompanied by increased chargeability - 20 millivolts/volt above the 10 millivolts/volt background. The source must be disseminated sulphides or graphite within a resistive host.

The overlap line is again remarkably similar in form and amplitude considering the distance separating the two energising current dipoles.

MIP on Line 2100N...The 18 millivolts/volt above background chargeability response observed at about 230W on the gradient EIP survey was repeated using MIP. The resultant anomaly showed a 6 milligamma/gamma internal polarization response whose source is calculated to be about 50 metres below surface. The decay form is *normal*. The H_N data shows the source to lie within a *resistive* host surrounded by more conductive material (e.g.

silicified sulphides within a more conductive non-silicified host).

Line 2300N is a dramatic departure in form of the chargeability profile from lines to the south. Save for a distinct 6 to 7 millivolts/volt anomaly at 262W (maximum depth to source 75 metres), the low chargeability background of about 2 millivolts/volt rises rapidly to the east of 075W, and to the west of 325W to over 20 millivolts/volt above this low background. Changes in rock type at about 075W and 325W must account for this phenomenon. The apparent resistivity data shows a sympathetic rise.

On both lines 2500N and 2700N the chargeability and apparent resistivity profiles show very similar general features, but in the case of 2700N the profile form is subdued. Increase in resistivity is accompanied by increase in chargeability. The very low chargeabilities together with low resistivities are considered to be due to weathering and oxidation over a conductive unit.

On line 2700N low chargeability was recorded between 400W (12 millivolts/volt) to 100W (8 millivolts/volt), after which it rises rapidly to 20 millivolts/volt at 00 in sympathy with a rise in apparent resistivity from 100 ohm-metres to 400 ohm-metres. A rock type change is suggested at 075W.

Similar form in chargeability was noted on line 2900N between 400W to 125W where the chargeabilities were a low 10(±) millivolts/volt, after which they rose to 25 millivolts/volt at 062W and at 012W reached 25 millivolts/volt again. A rock type change is again suggested at about 125W/130W.

The resistivity and chargeability picture on line 15900N is altogether different to that seen on lines to the south. This clearly indicates a quite different rock sequence on this line.

Accompanying low apparent resistivities of 10 ohm-metres at 512W are 100 millivolts/volt chargeabilitites. The depth to the massive graphite and/or sulphides and/or serpentine conductor at this point is about 10 metres.

Smaller responses of about 15 millivolts/volt above background were located at 562W and 612W accompanied by a 50% fall in apparent resistivity. The sources of these two responses are considered to be conductive, chargeable sources at maximum depths of less than 20 metres in both cases.

To the west, a truly significant decrease in apparent resistivity to 3 ohm-metres was accompanied by apparent chargeabilities of 98 millivolts/volt (and is open to the west). The maximum depth to this electrically continuous ("massive") graphite or sulphide source is 25 metres. The source should be ascertained.

To the east of 425W resistivities increase to reach 1000 ohm-metres at 300W after which they remain at this level. Chargeability within this zone varies between 10 and 50 millivolts/volt, with shallow disseminated sulphide (or graphite) sources being identified at 162W, 212W and 262W.

CONCLUSIONS

1 - The strike of all three properties of magnetics, apparent chargeability and apparent resistivity varies *around* grid north-south.

2 - Three "dislocations" trending grid north-east/south-west are proposed.

3 - All three physical properties show extreme variation within the survey area, and further, generally show distinct boundaries. This has enabled a good physical property map to be constructed which represents *some function* of the underlying geology.

4 - The positioning of the Kapi Fault is not easy in spite of a wealth of detailed information. Two suggestions are made, however, the author is convinced that detailed discussions between geophysicist and geologist after the area geologist has studied the various physical property maps and interpretation plans attached to this report, will lead to a more positive

placement of the fault.

5 - As the geological setting of each of the induced polarization maxima defined on this survey is unknown, each has been separately described. The possible nature of the source of each is described and the depth to source estimated. These responses show a wide variety of types from conductive to resistive. The maximum depths estimated vary to 75 metres but in general the sources lie between 25 and 50 metres.

The characteristics of each anomaly will be found under the detailed description of each line.

6 - The old mine workings centred at about 412W on line 1500N have a significant chargeability response from within an essentially disseminated source at 450W. This zone can be traced northwards across line 1700N at 425W, and continues across line 1300N just west of 350W. Should the old mine workings be of interest, then these responses should be investigated.

7 - Highly conductive conditions were noted just east of the old mine workings centred at 900N/362W, 1100N/337W. 1300N/325W, 1500N/350W and 1700N/337W *may* represent the position of the Kapi Fault. Chargeabilities over these resistivity lows also decline dramatically.

8 - In retrospect it would have been most helpful to have placed two current poles over the entire length of the grid, and measured H_N, so producing an H_N conductivity map over the whole area. Should the present data not be able to resolve the problems, it is strongly recommended that this be done.

9 - The increase in efficiency and data afforded by the use of the large 10/15KW generator for the EIP gradient survey was clearly demonstrated in this survey.

The author looks forward to discussing the results of this survey in the very near future.

Respectfully submitted on behalf of:

SCINTREX PTY. LTD.

A.W. HOWLAND-ROSE, MSc, DIC, AMAusIMM, FGS.

GEOPHYSICIST

035

SCINTREX MFM-3 High Sensitivity Vector Fluxgate Magnetometer

Function

The MFM-3 is a portable fluxgate magnetometer of unique design which performs vector magnetic field measurements in the milligamma region. It is especially useful in the study of micropulsations, in magnetotelluric surveying and in other magnetic field measurements requiring high sensitivity.

Features

- Resolution in the milligamma region
- Operates at ambient temperatures, no need for cryogenic conditions
- Single component measurement
- Three sensors can be combined to provide simultaneous three component measurements
- Flat frequency response far beyond the range of any other vector magnetometer
- Broadband
- Low inherent phase shift
- Rugged and lightweight for portable field use
- Low power requirements
- Dry cell or rechargeable batteries
- Ideal for magnetotelluric work

Applications

The MFM-3 was originally developed in conjunction with Scintrex's research in the MIP method. These instruments are in regular use in conjunction with standard Scintrex time or frequency domain induced polarization receivers and transmitters.

The MIP method has many advantages over normal EIP techniques under certain geological conditions, in particular in the presence of highly conducting surface materials. The MIP method is proprietary to Scintrex which is pleased to carry out MIP contract services on behalf of clients. Alternatively, Scintrex is prepared to license exploration groups to carry out MIP surveys.

Another use of the MFM-3 is to make measurements of magnetic fields related to "steady state" current flow in the earth created by a low frequency galvanically coupled transmitter. The information thus provided relates to the distribution of resistivities in the earth. The method has been termed "Magnetometric Resistivity". The results of such surveys can give conductivity information to great depths and have proven to be of use in geothermal as well as mineral exploration.

The flat frequency response of the MFM-3 to 1000 Hz, and its high sensitivity make it an excellent device for magnetic measurements in the application of the magnetotelluric method. The MFM-3 is the only non-cryogenic vector magnetometer with useful sensitivity in the milligamma range. It is low in power consumption and weight. It is therefore useful for making field measurements in remote areas, for the purposes mentioned above.

Technical Description of MFM-3 High Sensitivity Vector Fluxgate Magnetometer

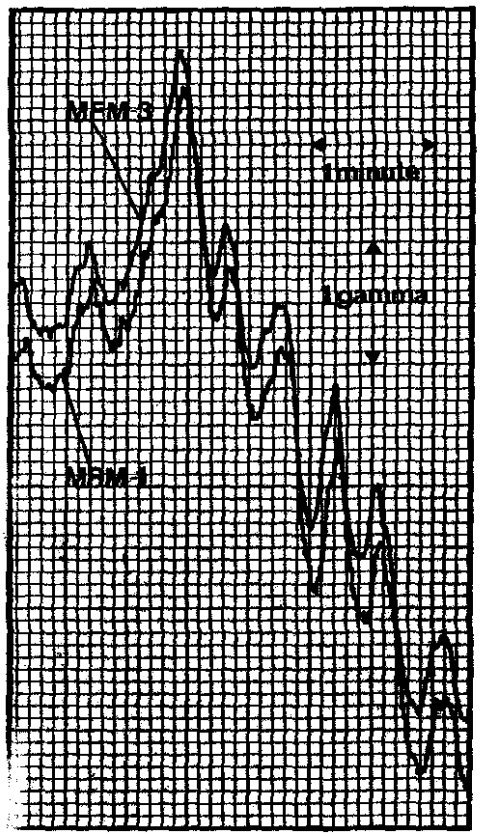

Comparative total field measurements using an MFM-3 oriented in the total field direction and a Scintrex MRM-1 Multiple Resonance Total Field Magnetometer reading once per second.

5 cm

Output Sensitivity	100mV/gamma ±2%
Output Dynamic Range	200 gamma
Output Impedance	50 ohms
Output Noise	0.01-1Hz: 10 milligamma peak-peak 1-1000 Hz: less than 1 milligamma RMS/√Hz
Frequency Response	0-1000 Hz (3 db point) 12 db/octave roll off
Meter Ranges	±10 and ±100 gamma full scale
Meter Scale	2 x 20 divisions, 64 mm long
Bucking Adjustments	Coarse 1:9 switched steps of approx. 10,000 gamma Coarse 2:9 switched steps of approx. 1,000 gamma Fine: 0-1,000 gamma by 360 turn potentiometer
Temperature Range	−40°C to +60°C
Temperature Drift	Less than 0.5 gamma/°C
Power Supply	12V DC rechargeable lead-acid snap-on battery pack
Power Requirements	Approximately 2.5 watts
Operating Time	Approximately 12 hours at 25°C
Connecting Cable	6 meters long
Dimensions	Console: 320x140x230mm Sensor: 810x140x140mm
Weight	Console: 4 kg Sensor: 5 kg Connecting Cable: 0.150 kg/meter
Options	Sensitivity at the output in the limits 10-500 mV/gamma Length of the cable connecting sensor to console up to 100 meters Dry cell non-rechargeable snap-on battery pack, or any 12V DC power supply.

Scintrex Limited
222 Snidercroft Road
Concord (Toronto) Ontario
Canada L4K 1B5
Tel: (416) 669-2280
Telex: 06-964570
Cable: Scintrex Toronto

Complete Geophysical Instrumentation and Services

SCINTREX PTY. LTD.
Formerly
SEIGEL ASSOCIATES AUSTRALASIA PTY. LTD.
GEOPHYSICAL CONSULTANTS AND CONTRACTORS

THE MAGNETIC INDUCED POLARIZATION METHOD

It is essential to grasp the very basic differences between the magnetic mode of acquiring induced polarization data *(MIP)* and the more conventional electrical mode *(EIP)*. As even geophysicists of some experience have difficulty in appreciating the full significance of the data obtained in the magnetic mode, I have incorporated into this report some remarks and comments on the main anomaly forms obtained from MIP.

The very brief description which follows is also designed to give a visual picture of the relationship between EIP and MIP, and demonstrate how the various MIP parameters of normalised horizontal magnetic field (H_N), chargeability *(M)*, secondary magnetic field (H_S) and decay rate *(ΔM)*, represent the electrical properties of the material over which the tests are made.

Comparison of the Electrical and Magnetic Modes of Acquiring Induced Polarization Data:- By far the most meaningful manner in which to visualise the nature of MIP (and indeed EIP) data, is to consider the *energy storage concept* and to look at the initial current flow patterns and the resultant equipotential field caused by the energising current, and then the consequent secondary current flow pattern and its associated secondary potential field caused by the decay of energy stored in the induced polarization phenomenon.

Energisation Process:- Normally current is applied to the volume to be sampled by means of two electrodes placed semi-parallel to the expected strike of the target mineralisation. In the diagram shown in Figure 1, the fine solid lines represent the current flow pattern so generated. The dashed faint lines represent the equipotential surfaces (lines in the section).

1031 WELLINGTON STREET, WEST PERTH, W.A. 6005
TELEPHONE 21 6934. TELEGRAMS "SCINTREX" PERTH

6 TRAMORE PLACE, KILLARNEY HEIGHTS, N.S.W. 2087
TELEPHONE 451 5367. TELEGRAMS "SCINTREX" SYDNEY

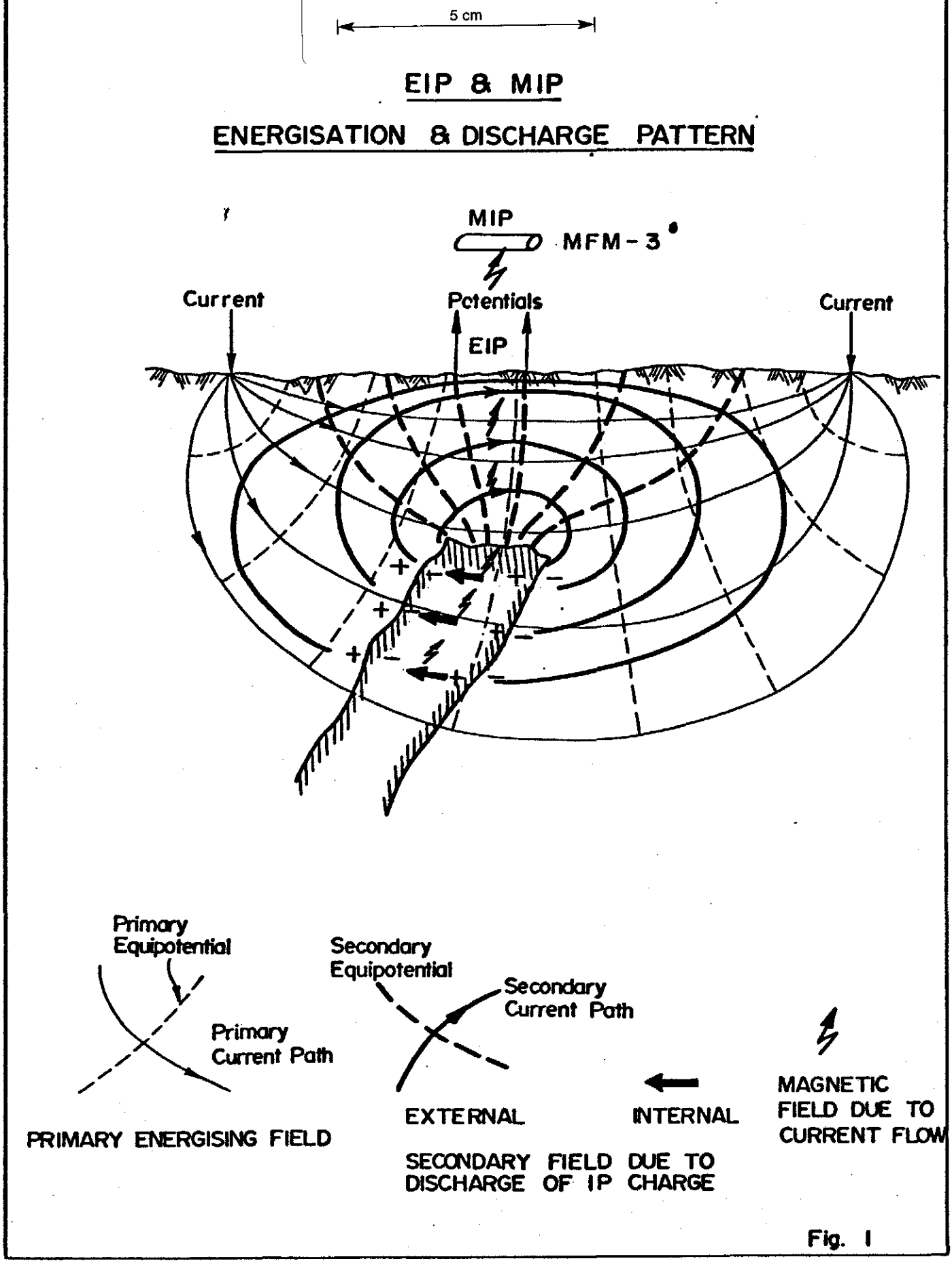
5 cm
EIP & MIP
ENERGISATION & DISCHARGE PATTERN
MIP
MFM-3
Current
Potentials
Current
EIP
Primary Equipotential
Primary Current Path
Secondary Equipotential
Secondary Current Path
PRIMARY ENERGISING FIELD
EXTERNAL
INTERNAL
MAGNETIC FIELD DUE TO CURRENT FLOW
SECONDARY FIELD DUE TO DISCHARGE OF IP CHARGE

Fig. 1

In the *electrical mode*, the two potential electrodes (See Figure 1) will measure the *resistivity* of a volume of material defined by the equipotential surfaces which are always at right angles to the current flow.

Energy Storage Process:- The material through which the current passes will store some portion of the energy in a way determined by the properties of the storage material. The amount of energy stored will depend on the total area of the sulphides (or graphite etc.) presented to the current, and thus, the greater this surface area with respect to the volume of material, the greater will be the energy stored. Finely disseminated material will store substantially more energy than coarse grained material.

The Discharge of Stored Energy:- On cessation of the energising current flow, the energy stored by the *chargeable source* will discharge *internally* within the source as shown by the solid arrows in Figure 1, and *externally* around the body in the medium surrounding the source as shown by the solid heavy lines in Figure 1. These currents are respectively known as *external* and *internal* current flow. The former is of *positive sign* as it is in the *same direction* as the original energising current, and the latter is *negative* in sign because it is in the *opposite direction* to the energising current.

In the electrical mode the discharge outside the body *ONLY* is investigated. In Figure 1 the thick solid lines show this discharge together with the *equipotential surfaces* (thick broken lines) which this current imposes. As with the charging process these surfaces must be at right angles to the current lines which impose them. The potential electrodes will therefore measure the stored energy (chargeability) as seen via the secondary

TYPICAL M.I.P. ANOMALY FORMS

THEORETICAL MODEL

CHARGEABLE SOURCE
NO RESISTIVITY
CONTRAST

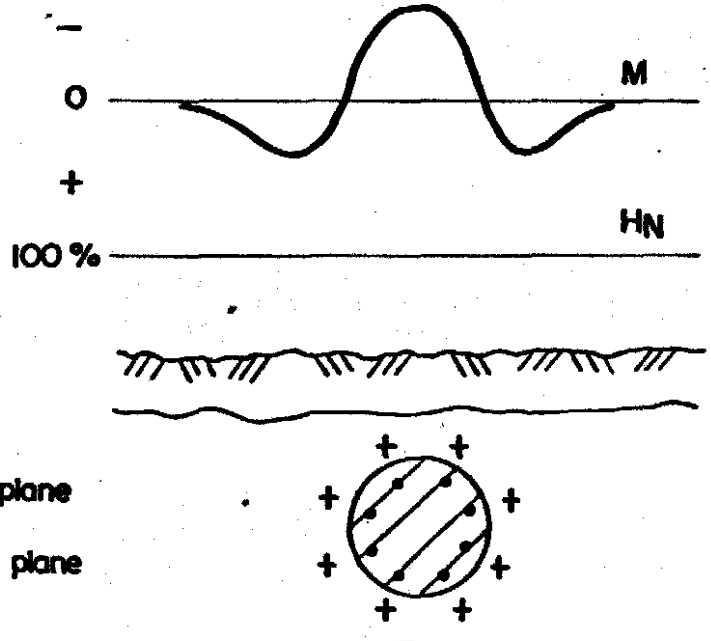

+ External current flow into plane of paper
• Internal current flow out of plane of paper

TYPE A

CHARGEABLE SOURCE
RESISTIVE SOURCE

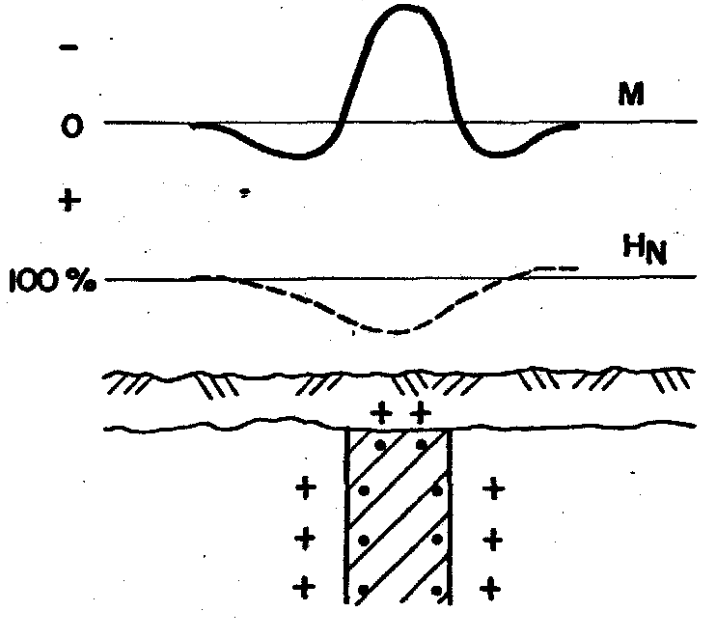

Fig. 2

equipotential field. It is important to note that *(i)* this is *NOT* the same volume as the resistivity measurements and *(ii)* it is *NOT* the original IP signal as stored by the body, but a measurement distorted and processed by the environment through which it passes.

In the *magnetic mode* a very sensitive magnetometer (Scintrex MFM-3) is used to "sense" the current flow both *inside* and *outside* of the *source material*. This occurs because each electron which flows in the ground carries with it an associated magnetic field. This magnetic field will pass *unhindered* through the environment and thus both the discharge *internally* and *externally* to the source can be monitored on the surface.

The Form of MIP Anomalies:- The enclosed Figure 2 demonstrates the theoretical form of an MIP anomaly from a source which has no electrical contrast with the enclosing material, but has the property of retaining charge. (In nature such anomalies are in fact observed over heavy mineral deposits in beach sands)

Energisation is along strike, out of the plane of the paper, by a gradient array. All diagrams represent the current flow into (crosses) and out of (dots) the plane of the paper due to a storage of electrical charge in the source. In Figure 2 over the source, the magnetometer will "see" a surplus of internal (negative) current flow, while on the flanks of the body, the external (positive) current flow will become predominant. The *"head and shoulders"* MIP anomaly shown is *always* seen over all sources. It is the distortions in shape, form and zero level that yield vital information as to conductivity of the source, conductivity of the environment above and about the source, the depth to the source and the nature of the mineralisation in and around the source.

TYPICAL M.I.P. ANOMALY FORMS

TYPE B

CHARGEABLE SOURCE
HOMOGENEOUS

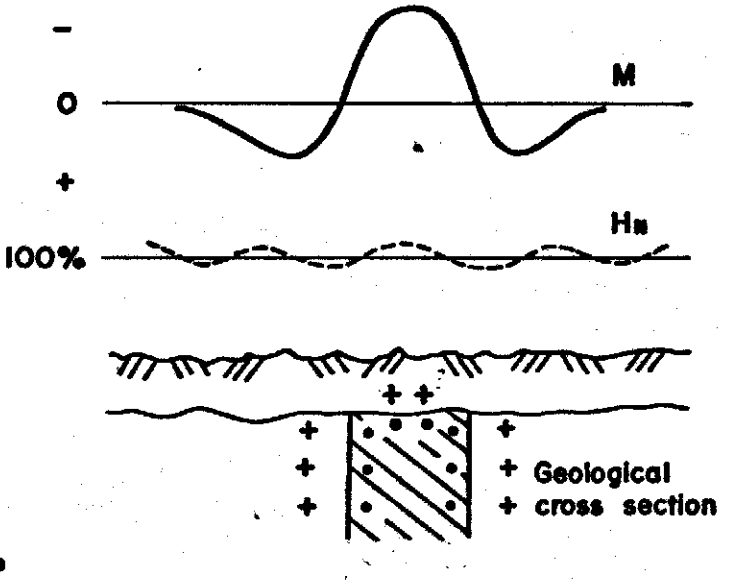

+ External current flow into plane of paper.

• Internal current flow out of plane of paper.

TYPE C

CHARGEABLE SOURCE
CONDUCTIVE

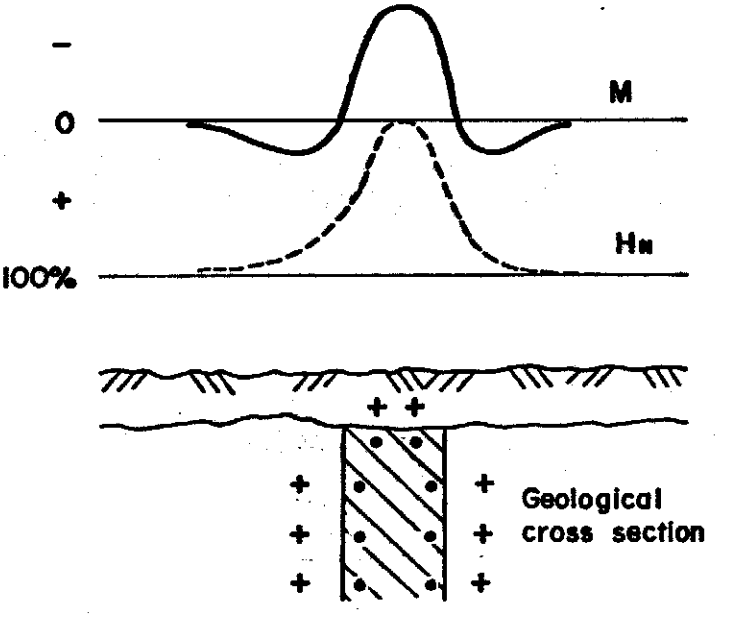

Fig. 3

In MIP the energising field is normalised, so that should the medium through which it passes be homogeneous, the resultant normalised horizontal field (H_N) will be 100% everywhere. Therefore, H_N in this "theoretical model" is everywhere 100%.

TYPE A (FIGURE 2) shows the typical anomaly form over a chargeable source which is more resistive than the surrounding medium. In such cases the normal *"head and shoulders"* anomalies coincident with a depression in the H_N are observed. An example of such an anomaly form is chalcopyrite/pyrite in quartz veins itself within a more resistive conductive rock unit.

TYPE B (FIGURE 3) In this case the chargeable source has no resistive contact with the enclosing material. This example is very similar to the theoretical model. An example of such an anomaly form would be over disseminated sulphides within a homogeneous rock unit.

TYPE C (FIGURE 3) In this case the source of the chargeable material is itself more conductive than the enclosing rock type. When the observed H_N values are *less than* 180% - 200%, a normal *"head and shoulders"* anomaly is observed over the source. In practice, observed H_N values rarely exceed 150% of normal.

TYPE D (FIGURE 4) In this most important anomaly form which invariably is associated with massive sulphides which are both conductive and electrically continuous, a massive sulphide *must* be surrounded by a disseminated halo within more resistive host rocks. In this case the disseminated sulphides will naturally store the induced polarization charge *far more efficiently* than the massive electrically continuous core. Thus, on completion of the energisation process, the charge stored within the disseminated halo will preferentially discharge through the conductive massive sulphide core. This effect has *NEVER* been

TYPICAL M.I.P. ANOMALY FORMS

TYPE D

CHARGEABLE SOURCE VERY CONDUCTIVE WITH DISSEMINATED HALO

+ External current flow into plane of paper.
• Internal current flow out of plane of paper.

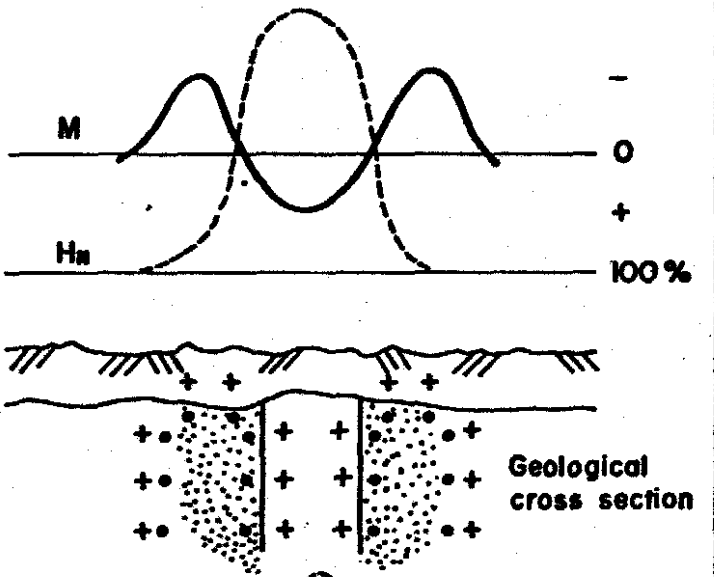

TYPE E

SOURCE VERY CONDUCTIVE BUT WITH LITTLE OR NO APPRECIABLE DISSEMINATED HALO

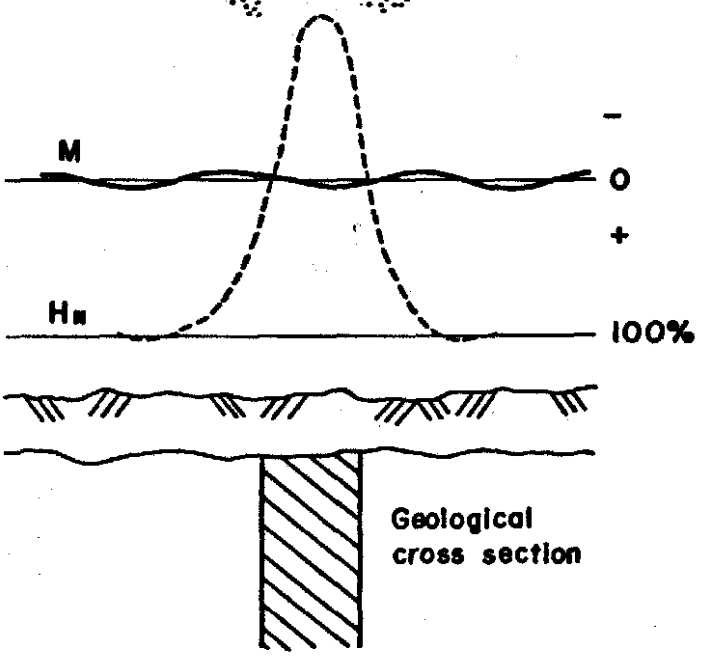

Fig. 4

observed where H_N values have been less than 180% of normal. This anomaly form due to its high H_N and coincident predominantly external (positive) current flow, is diagnostic when observed. An example of such a response is the Mt. Windarra pyrrhotite nickel, copper deposits in Western Australia.

TYPE E (FIGURE 4) Theory has always predicted that massive sulphides should show no IP effect, but invariably the disseminated material surrounding massive zones are sufficient to show the body up clearly. Over a number of Western Australian pyrrhotite nickel deposits, the massive, conductive, electrically continuous sulphides *are not* surrounded by any significant disseminated halo. Thus, little or no material is available for storing the induced polarization charge. However, the substantial normalised magnetic field which is invariably very high indeed (certainly in excess of 200% and as high as 400%) is the diagnostic feature. To date responses of such magnitude have never been observed over electrolytic conductors, even in the world's most conductive environments in Western Australia's salt lakes belt. However, such cases will inevitably be recorded therefore caution is needed in evaluating this rare anomaly type.

Modification of Anomaly Form by the Environment:- It is important to realise that each of the above anomaly forms is modified by the environment occurring immediately above the chargeable source. Two such cases are shown to illustrate the modification in the form of the chargeability anomaly which occurs. Both the sources show no contrast with the enclosing host material as per Type B.

In Type F (Figure 5) the source is covered by dessicated sands. Thus the return external current *cannot* flow above the body. Thus the external current flows *under* the source and/or around the sides of the source. The observed induced polarization

TYPICAL M.I.P. ANOMALY FORMS

TYPE F

CHARGEABLE SOURCE HOMOGENEOUS (AS B) UNDER DESSICATED RESISTIVE SAND COVER

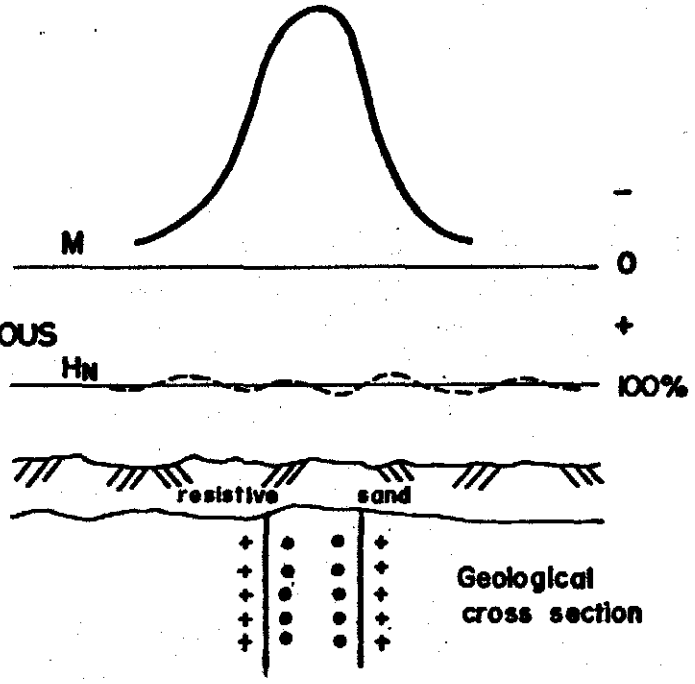

+ External current flow into plane of paper.
• Internal current flow out of plane of paper.

TYPE G

CHARGEABLE SOURCE HOMOGENEOUS (AS C.) UNDER HIGHLY CONDUCTIVE COVER

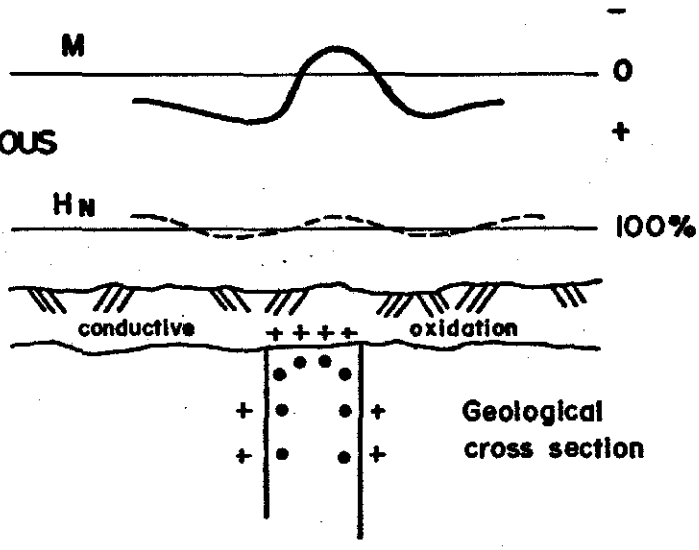

Fig. 5

anomaly observed via the magnetic sensor is invariably larger than normal as it is not reduced by external current flow above the body, and lacks the typical *"head and shoulders"* form. In addition the chargeability is usually entirely *internal* (i.e. negative).

In the case of *Type G* (Figure 5) the material between the source and surface is highly conductive. Some observed examples include relatively shallow, highly conductive salt lakes in Western Australia and, in the deep (100 metres) less conductive (5 to 10 ohm-metres) oxidation occurring in the Cobar area of New South Wales. In this case the characteristic features of the anomaly form are a much reduced *"shoulder"* level and a much reduced anomaly amplitude. The former occurs because of the preferential external current flow in the conductive overburden/ oxidation as a whole, and the latter due to the more intensive external current flow over the body itself.

Secondary Horizontal Magnetic Field (H_S) This parameter is also displayed, and is the magnetic field due to the discharge of the stored energy. Under certain conditions a study of H_S is more meaningful than M and H_N. However, in most cases it mirrors them.

The Significance of Decay Form (ΔM) Since the induced polariztion data was first studied in the laboratory, the variable nature of the decay of the stored IP charge with mineral composition and grain size has been known. However, rarely if ever, is this phenomenon observed in the field. There is in fact a very simple explanation as to why this is in fact so.

In *Figure 1* the energising current is shown in faint dashed lines. The resultant discharge (external and positive), is shown in

bold lines, while the internal negative discharge is seen in similarly bold arrows. The direction of the arrows indicates the direction of current flow.

Now, on the passage of the energising current, the material making up the chargeable source will store the energy in a way and a mode determined by that mineralisation. As the induced polarization effect is proportional to the *total surface area* presented to the passage of the energising current, very finely electrically continuous sulphides will store significantly more charge than will an equivalent value of coarsely disseminated material. Also should the grains be *finely* divided and/or *sharp grain boundaries*, or *platey* they will acquire the energy *rapidly* and on cessation of the energising current will discharge *rapidly*. Coarser grained material will take longer to charge and discharge than will fine grained material. Thus the speed at which the stored energy discharges can be a diagnostic feature. This is particularly true when mineralisation of markedly different form is required to be differentiated where other properties such as conductivity show no diagnostic difference.

As has been seen in Figures 2 to 5 the external (positive) chargeability above the body is characteristic of the internal current flow *within the body*. Thus the observed decay form is characteristic of the mode of the decay *within the body*.

In the case of electrical induced polarization, the energy stored in the body is observed on the surface *after it is discharged through the environment*. Thus as the discharge passes through the medium between the source and the surface the medium will, under normal circumstances, modify not only the amplitude of the signal but also the decay form thereof. In "normal" circumstances where the medium is both resistive and chargeable, the decay form observed via the electric mode

will be characteristic of the *medium* and *not the source*. However, as the intrinsic chargeability and resistivity of the medium approaches zero, the observed decay *will approach that of the source*. The decay form observed in the electric mode in highly conductive areas of intense oxidation such as Cobar New South Wales and Kalgoorlie, Western Australia approaches that of the source mineralisation, while over normal resistive cover the observed EIP decay form is always "normal". Therefore, only when induced polarization measurements are taken in the magnetic mode can the nature of the causative mineralisation's decay form be identified.

How Decay Information is Obtained:- The Scintrex IPR-8 induced polarization receiver is used in the time domain. This instrument records the chargeability at various times *after* the energising current is switched off and in this way records the rate at which the stored energy is discharged. The resultant recorded slices M_1, M_2, M_3, M_4, M_5, M_6 are then "normalised" by the receiver in such a way as to read $M_1 = M_2 = M_3 = M_4 = M_5 = M_6$ *if* the decay form is normal. Chargeable responses from finely grained mineral assemblages will be indirectly shown up in the field as $M_1 > M_2 > M_3 > M_4 > M_5 > M_6$, while coarser grained mineral assemblages will be shown up as $M_1 < M_2 < M_3 < M_4 < M_5 < M_6$.

In the display of the data ΔM is plotted where $\Delta M = |M_6| - |M_1|$. In this shortened presentation ΔM will be positive and large when "coarse grained" material is the source, 0 for "normal grain" size sources and large and negative for "fine grained" mineral assemblages.

The Importance of Frequency:- When induced polarization is carried out over a range of frequencies in the magnetic mode whether in terms of chargeability (time domain) or phase angle or frequency effect (in the frequency domain), a band of frequencies

is observed at which the maximum IP effect occurs. Frequencies above and below this band show a *reduced* effect. This *"peak frequency"* can be an important factor in whether the source material is seen clearly or not. The wholly electrically discontinuous disseminated deposits such as porphyry coppers have peak frequencies of 6Hz - 40Hz while massive electrically continuous coarse grained deposits occur low in the spectrum (less than 0.1Hz to 1Hz).

Much has to be learnt about this phenomenon (which is of course equivalent to decay form information), but it does indicate that the effective frequencies at which any IP (EIP or MIP) is carried out is important.

Other Significant Points:-

1 - The above remarks refer to time domain. However, measurements made in terms of frequency effect and phase angle in the frequency domain, show precisely the same phenomenon. There are distinct advantages in the application of MIP in the frequency domain, in particular the signal to noise ratio for a given transmitter is significantly greater with frequency. A disadvantage is that the effective "multi-frequency" approach of observing the decay form cannot be obtained without repeating the work at various frequencies.

2 - In several unique circumstances the method has vast superiority over other electrical methods. Firstly, in areas where the external (positive) current flow from the IP source cannot reach the surface either because of dessicated desert sands and/or due to a complete shorting out of the return signal at the base of a salt lake. Other cases where MIP is a unique solution is where chargeable material (even when weakly so) such as heavy minerals occur in barren quartz sands. In such circumstances EIP techniques

cannot be applied. One further application is when materially different mineral assemblages having markedly different decay forms are required to be differentiated.

3 - In applying the MIP method to exploration problems there are two characteristics problems to solve. The first is to clearly ascertain what are the range of characteristics of the target sources, and secondly to apply the method in an effective *and* efficient manner. This may mean commencing test work in the time domain and carrying out production surveys in whichever domain gives the greatest efficiency.

A.W. HOWLAND-ROSE, MSc,DIC,AMAusIMM,FGS.

SCINTREX PTY. LTD.

SCINTREX PTY. LTD.

Formerly

SEIGEL ASSOCIATES AUSTRALASIA PTY. LTD.

GEOPHYSICAL CONSULTANTS AND CONTRACTORS

SCINTREX IPR-8 INDUCED POLARIZATION

TIME DOMAIN RECEIVER

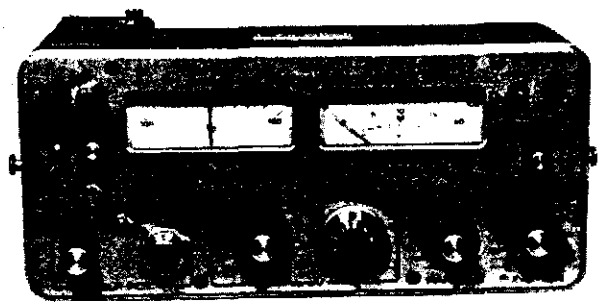

1031 WELLINGTON STREET, WEST PERTH, W.A. 6005
TELEPHONE 21 6934. TELEGRAMS "SCINTREX" PERTH

6 TRAMORE PLACE, KILLARNEY HEIGHTS, N.S.W. 2087
TELEPHONE 451 5367. TELEGRAMS "SCINTREX" SYDNEY

I INTRODUCTION

The basic equipment required for an Induced Polarization survey consists of a transmitter, a receiver, wire and electrodes.

Most time domain induced polarization transmitters transmit square waves with equal "on" and "off" times. Polarity is automatically changed between the pulses. The waveform shown below indicates how the current is usually transmitted. The pulse times range from 1 to 8 seconds.

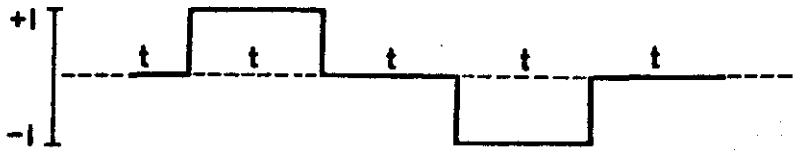

FIGURE 1A

The transmitter is powered by batteries (portable type units or a motor driven generator. Scintrex manufactures various time domain induced polarization transmitters ranging in power from 25 watts to 15 kW. The choice of a transmitter depends on various factors such as: the electrode spacings to be employed, contact resistance and the resistivity of the subsurface. The IPR-8 receiver is designed for use with any time domain induced polarization transmitter.

The IPR-8 time domain induced polarization receiver is of the state-of-the-art design, packaged in a rugged and portable manner. Using integration and automatic normalization, it measures the characteristics of an induced polarization decay curve set up by overvoltage and other effects occurring in rocks. When induced polarization effects (such as due to metallic-non metallic interfaces in rocks) occur, the waveform received at the receiver is not the same square wave as transmitted by the transmitter. The waveform shown below indicates the sort of wave distortion which is caused by the induced polarization phenomena.

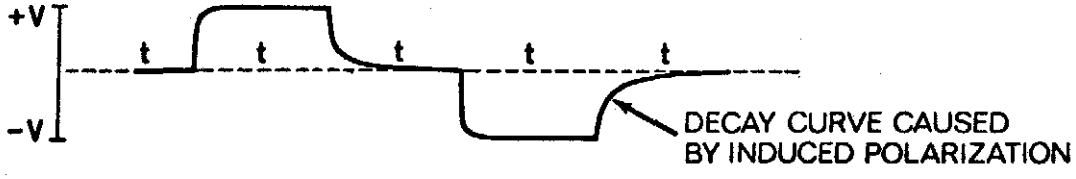

FIGURE 1B

II SPECIFICATIONS

The IPR-8 has the following specifications:

Input Impedance	3 megohms
Primary Voltage (Vp) Range	300 microvolts full scale to 40 volts full scale in 10 ranges
Accuracy of Vp Measurement	±3% of full scale
Vs/Vp Ranges	20 and 100 mV/V full scale
Vs/Vp Accuracy	±3% of full scale
Primary SP Buckout Range	±1 volt
Accuracy of SP Measurement	±3%, ±5 mV
Automatic SP Tracking Range	6 x Vp, maximum ±1 volt
Continuity Meter Reading	0 - 500 k ohms
50 or 60 Hz Powerline Rejection	-50 db (300x)*
Low Pass Filter	6 db/octave with fc = 20 Hz and 12 db/octave with fc = 36 Hz
Required Stability of Transmitter Timing	Need only exceed measuring program selected (1 or 2 seconds)
Operating Temperature Range	-30°C to +60°C
Dimensions	320 mm x 135 mm x 160 mm
Weight, Complete with Lid and Batteries	3.6 kg
Power Supply	4 D cells - Eveready No. 1050 or equivalent; estimated battery life 2 months intermittent duty at 25°C 1 Alkaline cell Eveready No. E91 or equivalent; estimated life 1 year

* 50 or 60 Hz depending on power system.

III QUANTITIES MEASURED BY THE IPR-8

Figure 2 shows the different parameters measured by the IPR-8. The usual measurements are Vp, the received primary voltage and "M", a parameter related to the transient curve. The Vp measurement is used in resistivity calculations while M is the chargeability (induced polarization) parameter. In addition, absolute values of the self-potential (SP) can be measured.

In all cases, the M quantity measured by the IPR-8 is the mean value of the transient voltage over a selected time interval to which the following normalizations have been applied:

- normalization for the length of the integration interval
- normalization for the primary steady state voltage (Vp)
- normalization for curve shape
- normalization for number of pulses

The units of the quantities measured are, therefore, dimensionless and are normally expressed in "millivolts per volt".

In the various modes of operation the transient voltage following the interruption of the primary current pulse is either integrated over one long period of time or sliced into either 3 or 6 slices. By using 6 slices, a good record of the decay curve shape can be obtained. The 3 slice mode gives some curve shape information and provides an economical standard mode in which to operate. The centre slice of this mode is reasonably close to the measurement made by the Scintrex IPR-7 and other receivers of the "Newmont Type", while the first and last slices can be used for a rapid check of curve shape. A more precise relationship is, however, presented later in this section.

Figure 2 shows the actual times used. For the receiver to operate, the transmitter timing may be any time period of one second or greater (i.e. $t \geq 1$ second) although transmitter and receiver timings of 2 seconds are considered normal for most surveys. Equal on and off timing assures the best noise rejection as the signal is averaged over the longest possible time, and the automatic self-potential adjustment is made closest to the reading time.

With the receiver set at $t = 1$ second, the decay ($\delta/2$) from the current-off time to the commencement of the measurement is 65 milliseconds and the slice width (δ) is 130 milliseconds. With the receiver set at $t = 2$ seconds the delay is 130 milliseconds and the slice width is 260 milliseconds. Fuller information on the programs is available from the tables in Figure 2.

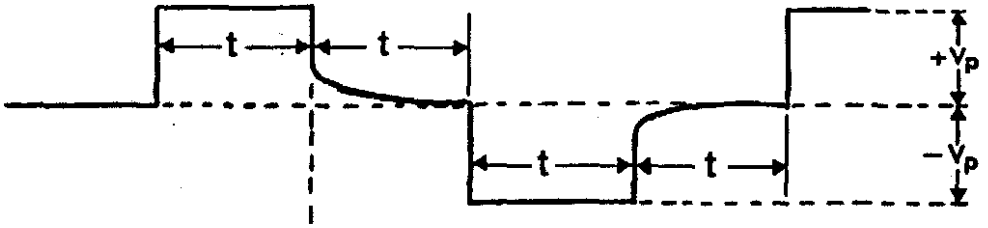

WAVE FORM AT INPUT TERMINALS

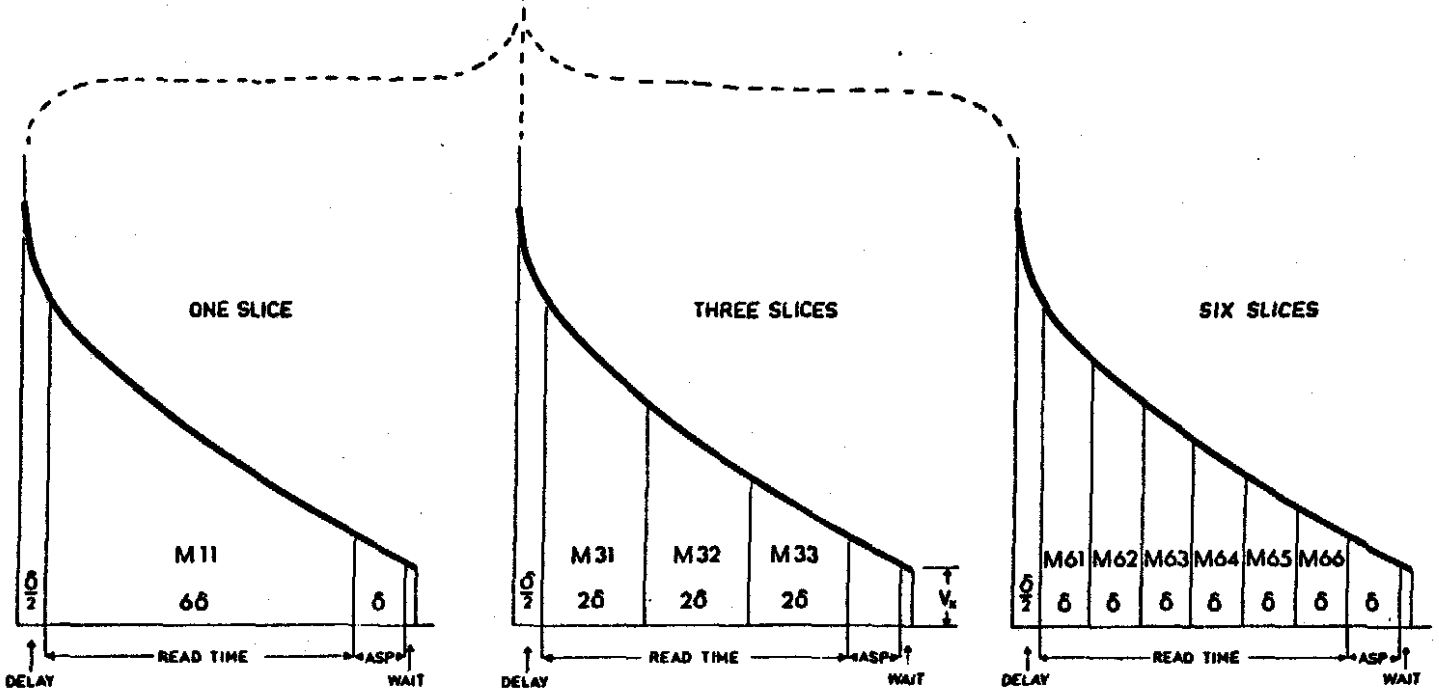

SECONDARY DECAY CURVE SHAPES AS APPLIED TO THE INTEGRATORS

t sec.	δ	delay time	waiting time	M 11				M 31			M 32			M 33			length
				from	to	mean	length	from	to	mean	from	to	mean	from	to	mean	
1	130	65	25	65	845	455	780	65	325	195	325	585	455	585	845	715	260
2	260	130	50	130	1690	910	1560	130	650	390	650	1170	910	1170	1690	1430	520

t sec.	M 61			M 62			M 63			M 64			M 65			M 66			length
	from	to	mean	from	to	mean	from	to	mean	from	to	mean	from	to	mean	from	to	mean	
1	65	195	130	195	325	260	325	455	390	455	585	520	585	715	650	715	845	780	130
2	130	390	260	390	650	520	650	910	780	910	1170	1040	1170	1430	1300	1430	1690	1560	260

FIGURE 2

PARAMETERS MEASURED WITH TIMES OF RECEIVER PROGRAM IN MILLISECONDS.

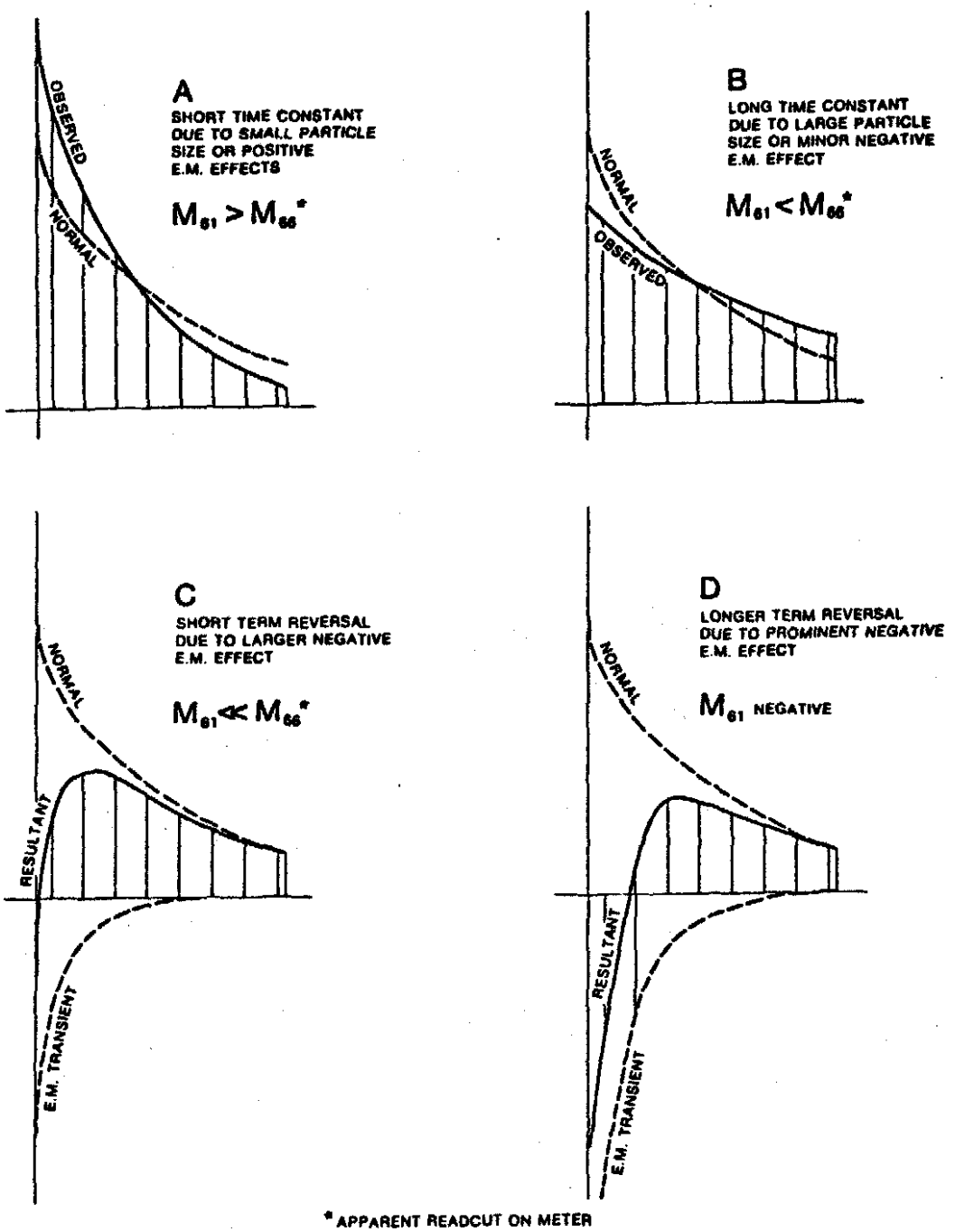

FIGURE 3

THE SIGNIFICANCE OF CURVE SHAPE INFORMATION GAINED USING 6 SLICE READINGS.

Each integration is normalized with respect to the Standard Induced Polarization Decay Curve which has been established by Newmont Exploration Limited. (ref. Dolan and McLaughlin in bibliography) This is achieved by choosing the sensitivities of the integrators so, that if the curve shape is normal, all slices within a given mode show the same amplitude of measurement. A further normalization is built in for the slice width, be it full, one-third or one-sixth of the total integration period. The net effect is that the reading will be the same regardless of the slice measured, providing that a standard transient decay curve form is present and that the same measuring cycle is used for transmitter and receiver (1 second or 2 seconds). Any departure from this standard curve form will be immediately obvious to the operator, without performing any calculations. For instance, a steeper decay will give a higher reading on earlier slices than on later slices. Reconstruction of the actual decay curve is easily effected by using the correction factors given in Table 1.

The shape of a time domain induced polarization decay curve can be altered by electromagnetic or interline coupling, by variations in the average size or degree of interconnection of the metallic particles in the bedrock or by other I.P. sources. Figure 3 illustrates the advantage of breaking the decay curve into slices. Utilizing only one wide slice, there is no indication of the shape of the decay curve. Positive electromagnetic coupling effects or small particle size may give rise to an abnormally short time constant (Case A) which, for multi-slice modes will be indicated by higher normalized readings of the earlier slices with respect to the later slices. An increase in the later slices over the earlier ones (Case B) may imply a longer time constant due to a minor negative EM transient or I.P. responses from large metallic particles, etc. Cases C and D, where the values of the initial slices are considerably reduced or are even negative, show the effect of negative EM transients of increasing amplitude.

A system of symbols has been created to indicate each of the measurable slices.

The general symbol is M_{txy} where:

- t is the timing chosen (i.e. 1 or 2 seconds)
- x is the number of slices in the mode chosen (i.e. 1, 3 or 6)
- y is the number of the slice referred to (i.e. 1, 2, 3, 4, 5 or 6)

Wherever two subscripts only are given, eg. M_{32}, it is understood to apply equally for t = 1 sec. or t = 2 sec.

A chargeability reading is defined by the following formula:

$$M = \frac{V_s \cdot 1000}{V_p} \quad \text{in mV/V}$$

where $$V_s = \frac{t_1 \int^{t2} V_s \, dt}{t_r} + V_x$$

and t_1 = time at beginning of slice

t_2 = time at end of slice

V_x = residual transient voltage at the end of the automatic self potential correction

$t_r = t_2 - t_1$, i.e. the integrating period

Chargeability values, uncorrected for curve shape, can be easily calculated if required. Normalizations for all slices are made using the M_{232} value as reference. In other words, there is no curve shape normalization applied to this slice; the M_{232} readout is, therefore, directly as measured. The same statement holds for the M_{132} slice, however, its value is one-half the value for M_{232} provided that the transmitter timing matches the receiver timing.

To restore the true transient curve shape (M true), the observed M readings (M read) are multiplied by the factors in Table 1.

TABLE 1

$$M_{true} = M_{read} \cdot k_1$$

Slice	k_1	
M_{11}	1.09	
M_{31}	1.47	
M_{32}	1.00	← NORMAL
M_{33}	0.81	
M_{61}	1.68	
M_{62}	1.27	
M_{63}	1.06	
M_{64}	0.94	
M_{65}	0.85	
M_{66}	0.78	

For the ideal "normal" I.P. transient curve form $M_{2xy} = 2M_{1xy}$ where M_{2xy} is for a 2-second on-off transmitter cycle and M_{1xy} is for a 1-second on-off cycle. The relationship between readings taken with differing transmitter and receiver timings is more complicated, particularly if the curve shapes are not normal.

Table 1 still applies for the case where the transmitting times are longer than the receiving times in order to reconstruct the relative curve shape.

Relationship between IPR-8 and
"Newmont Type" Receiver Measurements

The "Newmont Type" receivers (eg. Scintrex IPR-7) integrate the area under the transient curve from 0.45 seconds to 1.1 seconds. This is then multiplied internally be an instrumental factor to obtain the chargeability M in milliseconds.

For a normal decay curve form, the approximate relationship between the IPR-8 measurements and the Newmont Type chargeability is given by M_{232} (in mV/V) = M_N (in milliseconds) • 0.7.

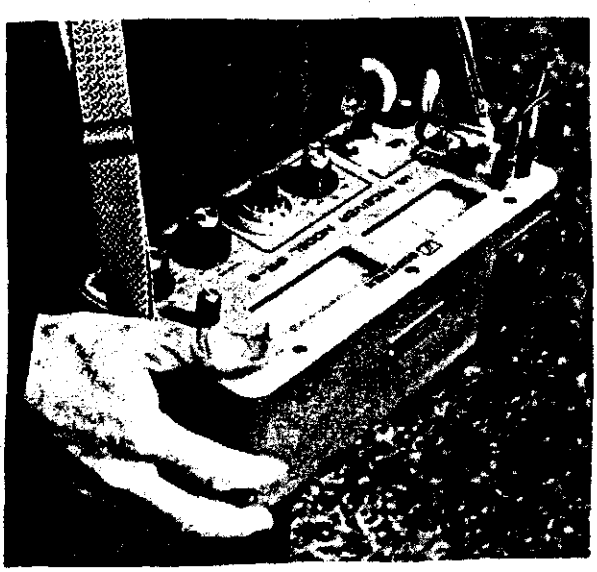

5 cm

LINE 1900 N

KARI GRID
Job: TAS-037

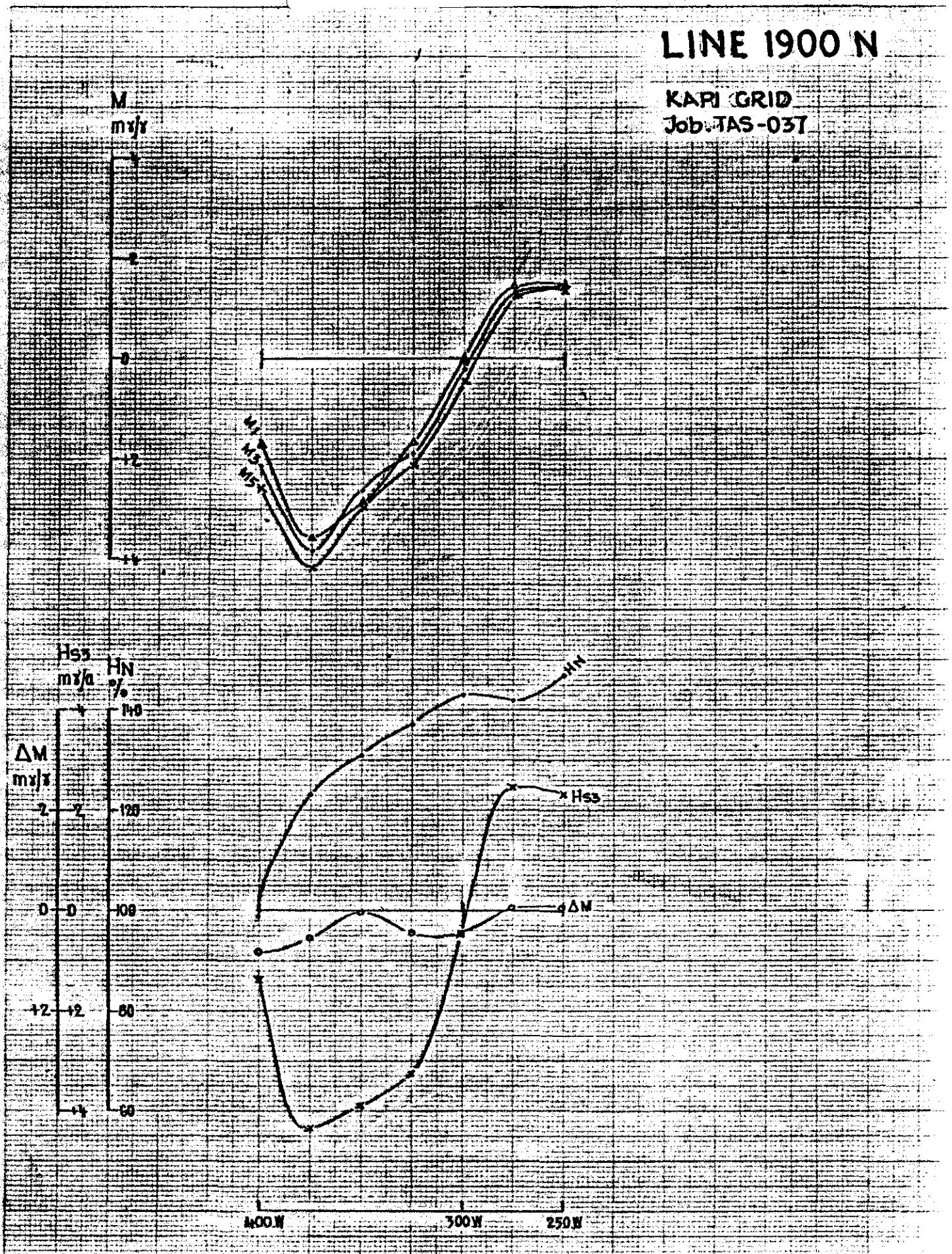

53

5 cm

317065

LINE 2100 N

KAPI GRID
Job. TAS-037

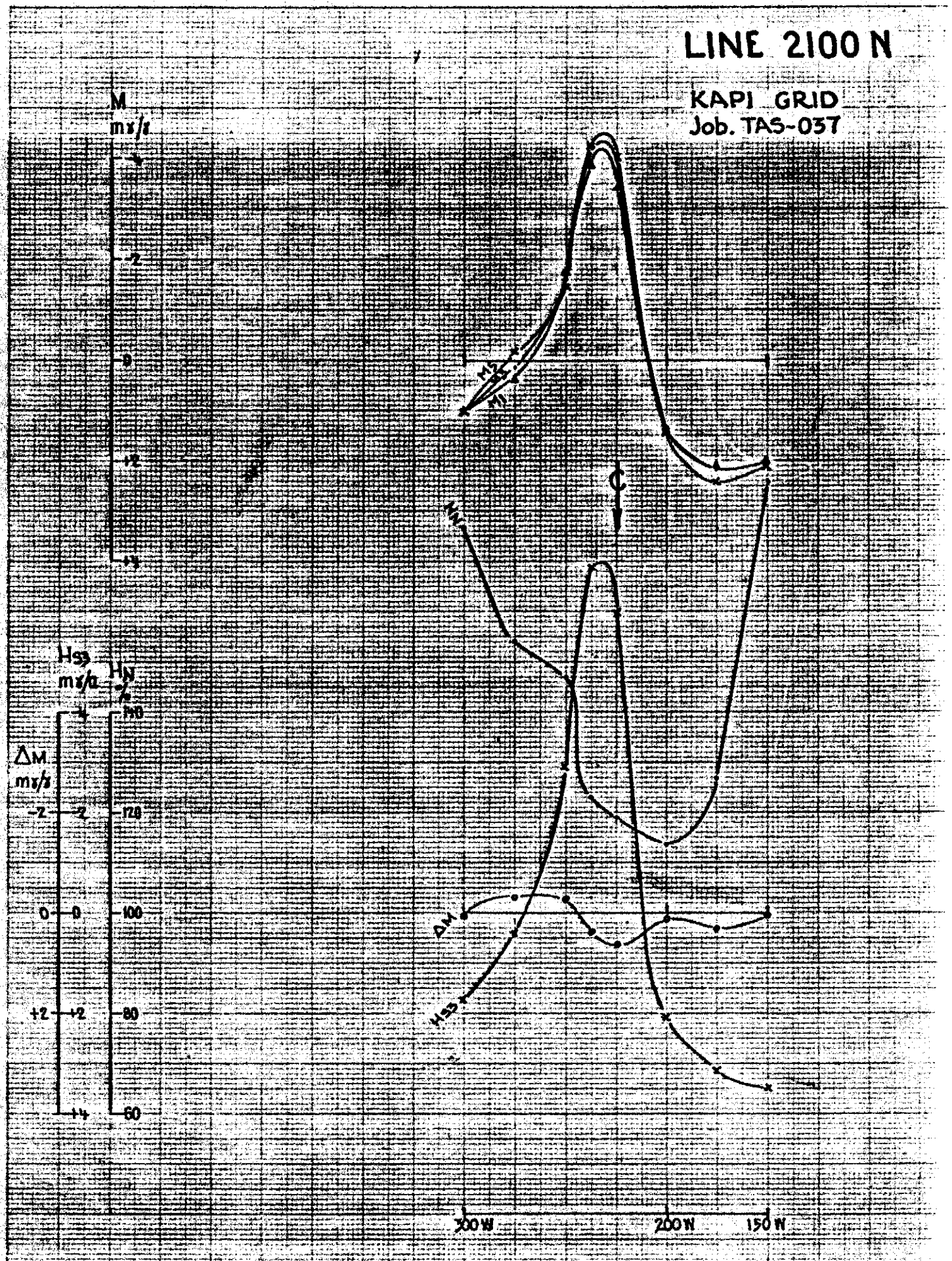

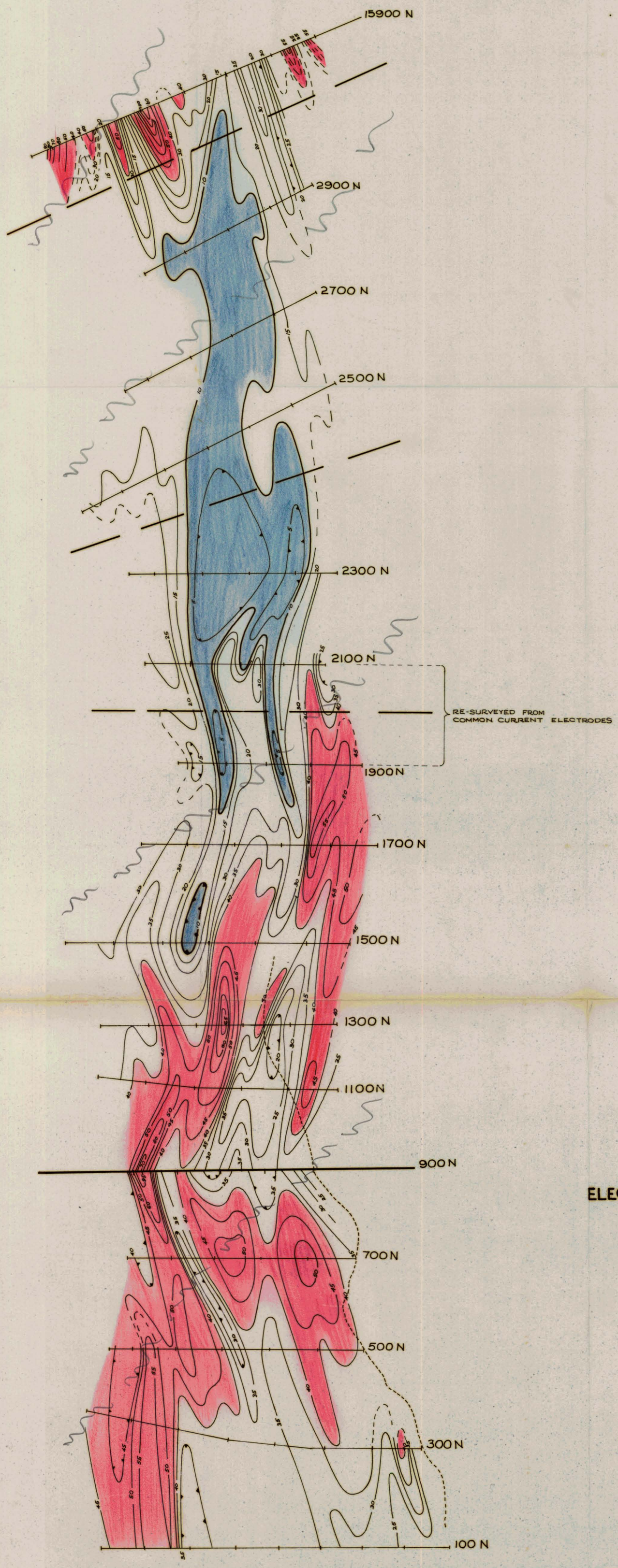

Legend

Gradient block boundary — —

Chargeability contours in millivolts/volt

RENISON LIMITED

KAPI GRID

WEST COAST - TASMANIA

ELECTRICAL INDUCED POLARIZATION SURVEY
GRADIENT ARRAY
CHARGEABILITY CONTOUR PLAN

5 cm

SURVEYED & COMPILED BY
SCINTREX PTY. LTD.

FEBRUARY 1977

200 100 0 100 200

SCALE. 1:5000 Metres

77-1207. 317066

Job Nº TAS-037 Sheet 1of 1 1500 PLATE 2

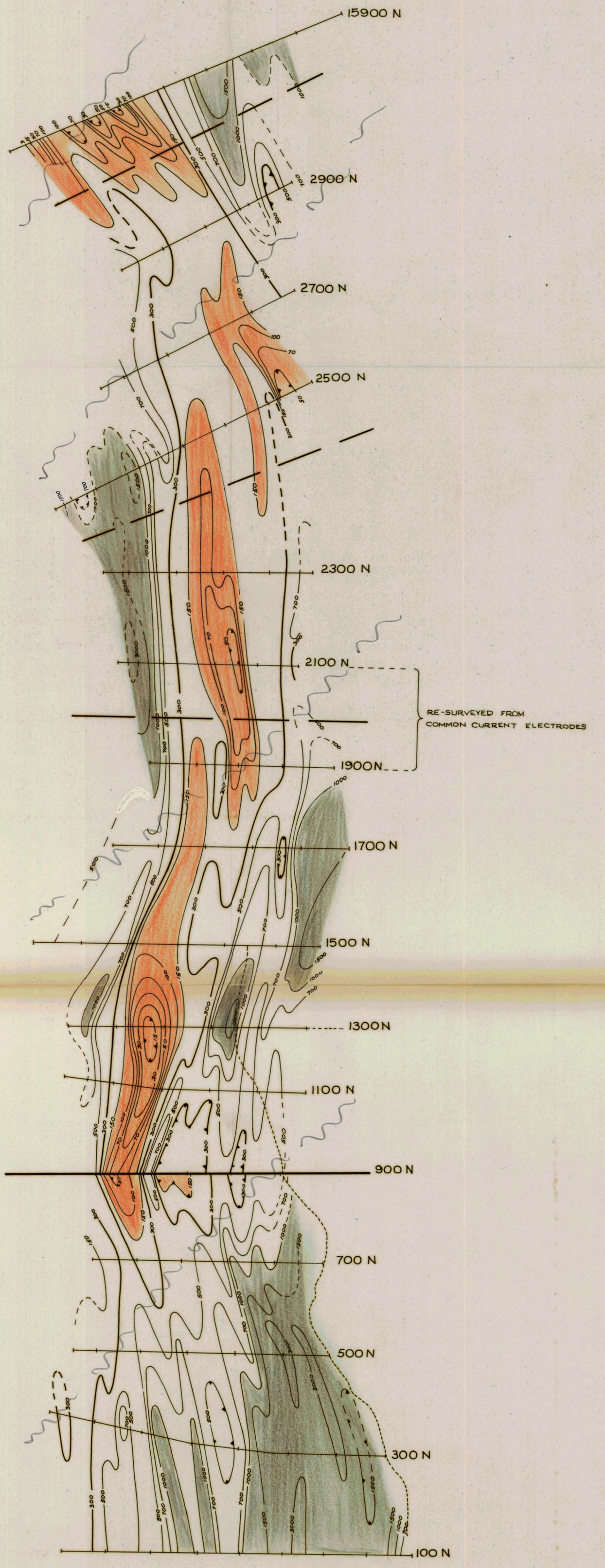

Legend

Gradient block boundary ——— ———

Resistivity contours in ohm-metres

RE-SURVEYED FROM
COMMON CURRENT ELECTRODES

RENISON LIMITED

KAPI GRID

WEST COAST - TASMANIA

ELECTRICAL INDUCED POLARIZATION SURVEY
GRADIENT ARRAY
RESISTIVITY CONTOUR PLAN

5 cm

SURVEYED & COMPILED BY
SCINTREX PTY. LTD.

FEBRUARY 1977

200 100 0 100 200

SCALE 1:5000 metres

77-1207.

317067

Job Nº TAS-037 Sheet 1 of 1 1501 PLATE 3

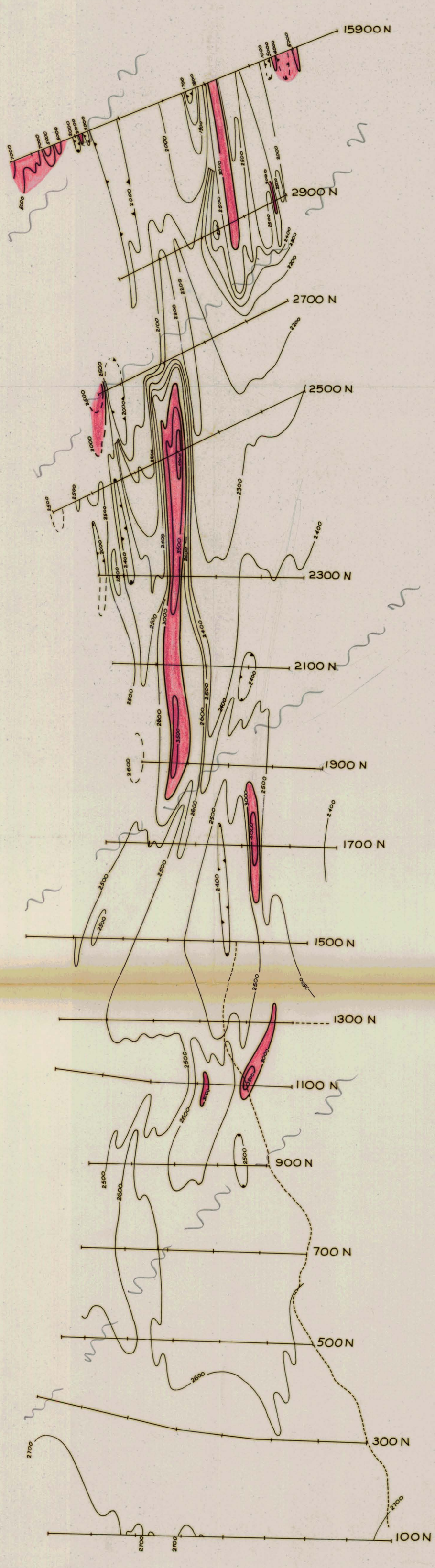

Legend

For correct total magnetic field add 60,000 gammas to all values.

RENISON LIMITED

KAPI GRID
WEST COAST - TASMANIA

TOTAL FIELD MAGNETOMETER SURVEY CONTOUR PLAN

5 cm

SURVEYED & COMPILED BY
SCINTREX PTY LTD.

FEBRUARY 1977

317068

200 100 0 100 200

SCALE 1:5000 metres

77-1204

Job Nº TAS-037 Sheet 1 of 1 1502 PLATE 4

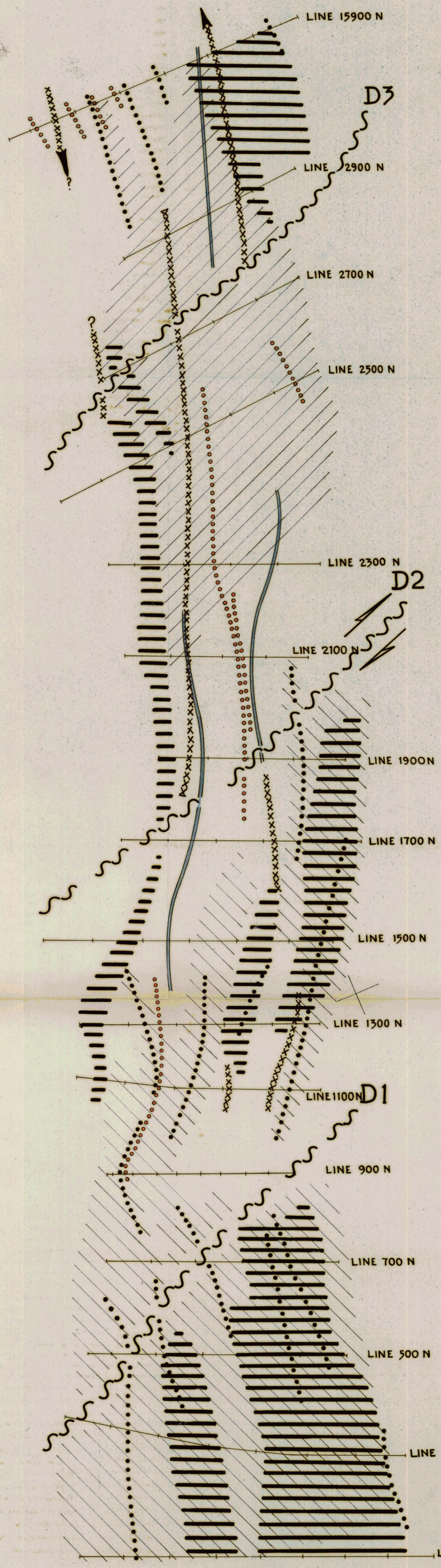

LEGEND

- Magnetic Highs
- E.I.P Highs
- E.I.P Lows
- Resistivity Highs
- Resistivity Lows
- Dislocations

RENISON LIMITED

KAPI GRID

WEST COAST - TASMANIA

ELECTRICAL INDUCED POLARIZATION SURVEY

SUMMARY OF GEOPHYSICAL PROPERTIES

5 cm

SURVEYED & COMPILED BY
SCINTREX PTY., LTD.

FEBRUARY 1977

317069

77-1204.

200 100 0 100 200

Scale - 1:5000

Job No. TAS-037 Sheet 1 of 1 1503 PLATE 5

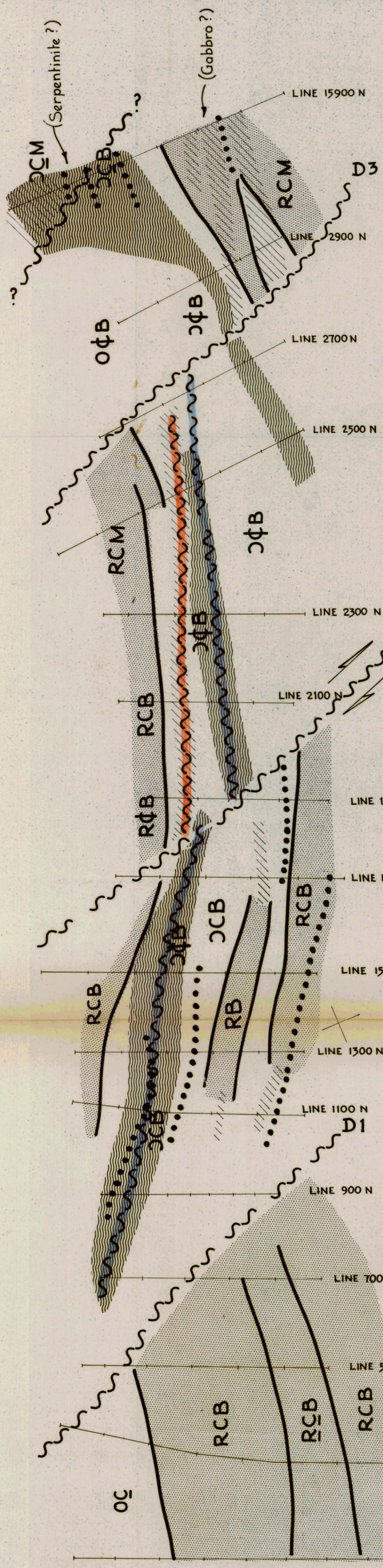

LEGEND

- Resistive
- Conductive
- Distinct Magnetic Highs
- E.I.P Highs
- Dislocations
- Kapi Fault (first suggestion)
- Kapi Fault (alternative)

Resistivity	Chargeability	Magnetics
R = resistive	C = chargeable	M = high
C = conductive	Ø = non-chargeable	B = background
O = intermediate	O = intermediate	

— extreme conditions e.g. R = extreme resistivity

RENISON LIMITED

KAPI GRID

WEST COAST – TASMANIA

ELECTRICAL INDUCED POLARIZATION SURVEY

INTERPRETATION PLAN

5 cm

SURVEYED & COMPILED BY
SCINTREX PTY. LTD.

FEBRUARY 1977

317070

200 100 0 100 200

SCALE 1:5000 Metres

77-1207

Job Nº TAS-037 Sheet 1 of 1 1504 PLATE 6

317071

MICROFILMED

EIP AND MIP SURVEY

KAPI GRID

ON BEHALF OF

RENISON LIMITED

FIELD DATA PROFILES

E.L. 42/71

Plate 1.

IN

Remove Note

083

317072

LINE 100N

JOB NO - TAS-037

DATE ~ 14-2-77

AREA ~ KAPI

EID TIME DOMAIN - 2SEC

C_1C_2 = 2600m

P_1P_2 = 25m.

590 595

C_1

M_3

CREEK

CREEK

R

R

M_3

5 cm

CHARGEABILITY in milli volts per volt.

50 45 40 35 30 25 20

RESISTIVITY in ohm-metre

1000 100 10

800W 600W 400W 200W 0W

10 5663
MILLIMETERS

082

317073

LINE 300N

JOB NO -TAS-037

DATE - 14-2-77

AREA - KAPI

R.I.P TIME DOMAIN -2SEC

C_1C_2 = 2400m

P_1P_2 = 25m.

5 cm

CONDUCTIVITY in millimhos per unit

50

40

30

1000

20

RESISTIVITY IN ohm metres

100

10

R

M_3

700W 600W 400W 200W 0

MILLIMETERS

081

317074

LINE 500N

JOB NO. — TAS 037
DATE — 14-2-77
AREA - KAPI
EIP Time Domain - 2sec
C_1C_2 = 2400m
P_1P_2 = 25m.

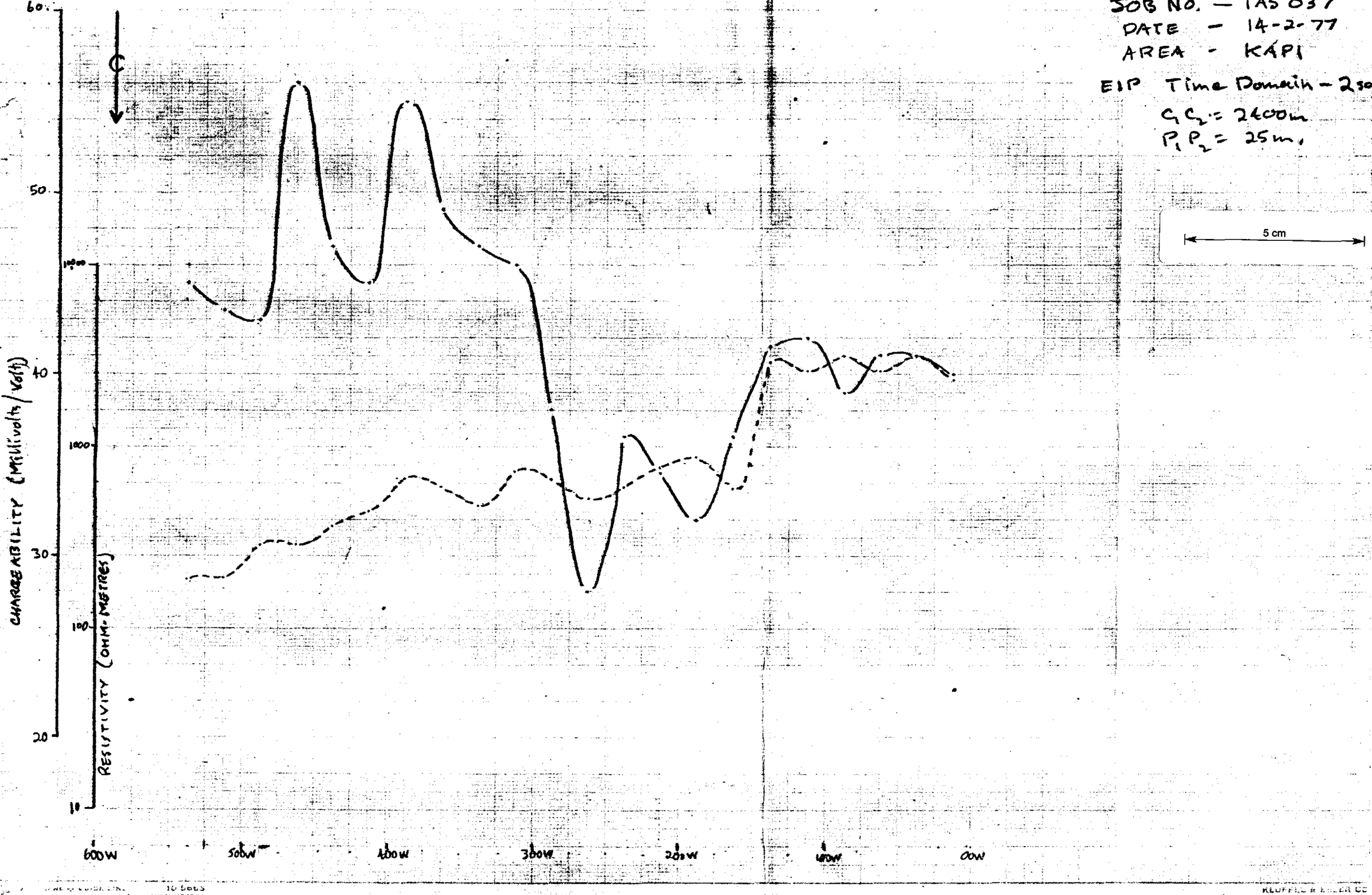

080

317075

LINE 700N

JOB No TAS-037

DATE ~14-2-77

AREA KAPI

EIPTIME DOMAIN 2SEC

C_1C_2 = 2400m

P_1P_2 = 25m

5 cm

CHARGEABILITY IN MILLISECS PER VOLT.

50

40

30

M_3

R.

RESISTIVITY IN OHM-METRES

1000

100

10

500W

400W

200W

00.

079

317076

LINE 900N

JOB N°: TAS-037

DATE : 77-02-12

AREA : KAPI

EIP TIMEDOMAIN(2S)

$C_1 - C_2$ = 2800m

$P_1 - P_2$ = 25m

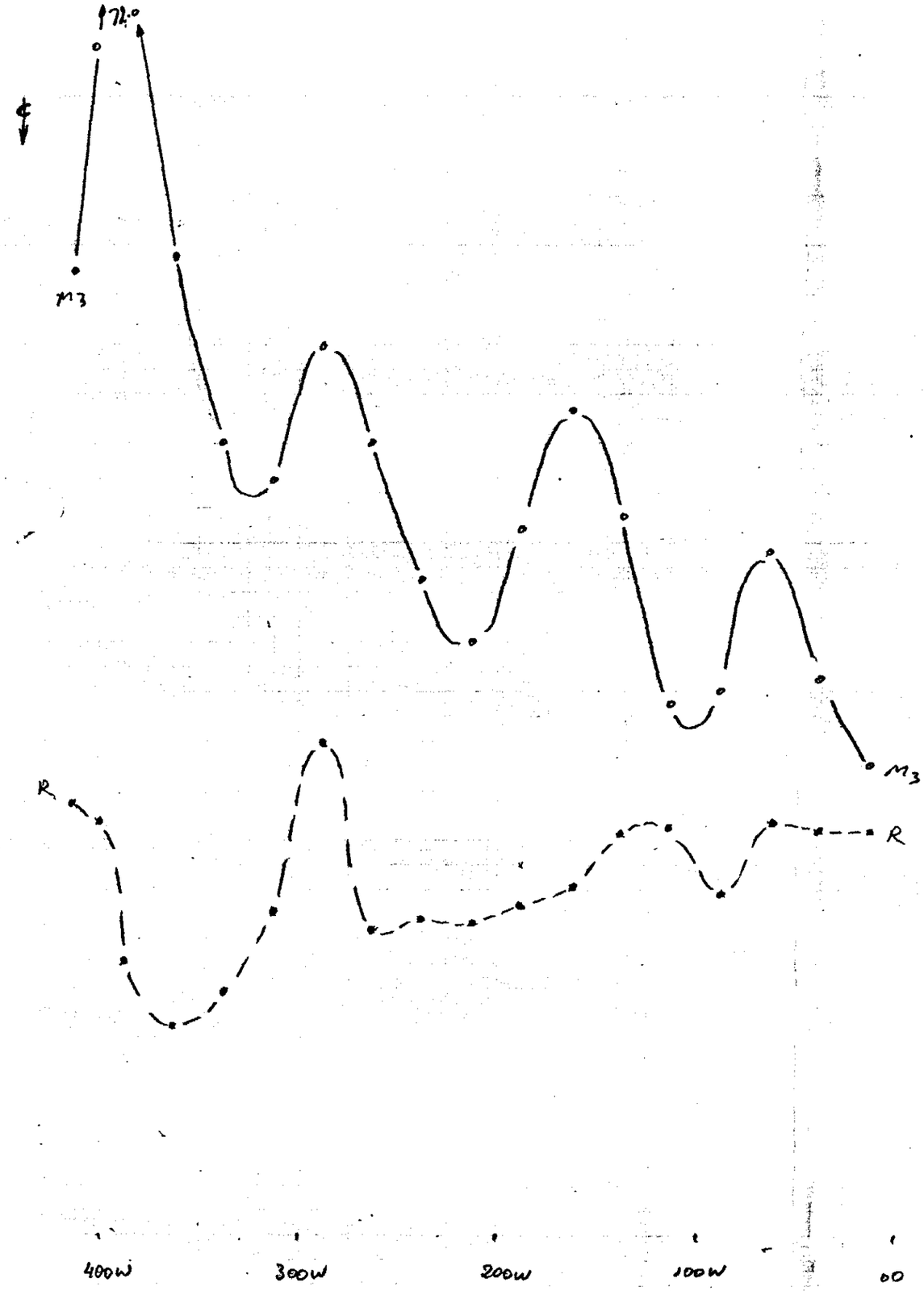

5 cm

078

317077

LINE 900N. (OVERLAP)

JOB No ~ TAS 037

AREA ~ KAPI

DATE ~ 14/2/77

EIP TIME DOMAIN 2sec.

C_1C_2 = 2400ms

P_1P_2 = 25ms.

5 cm

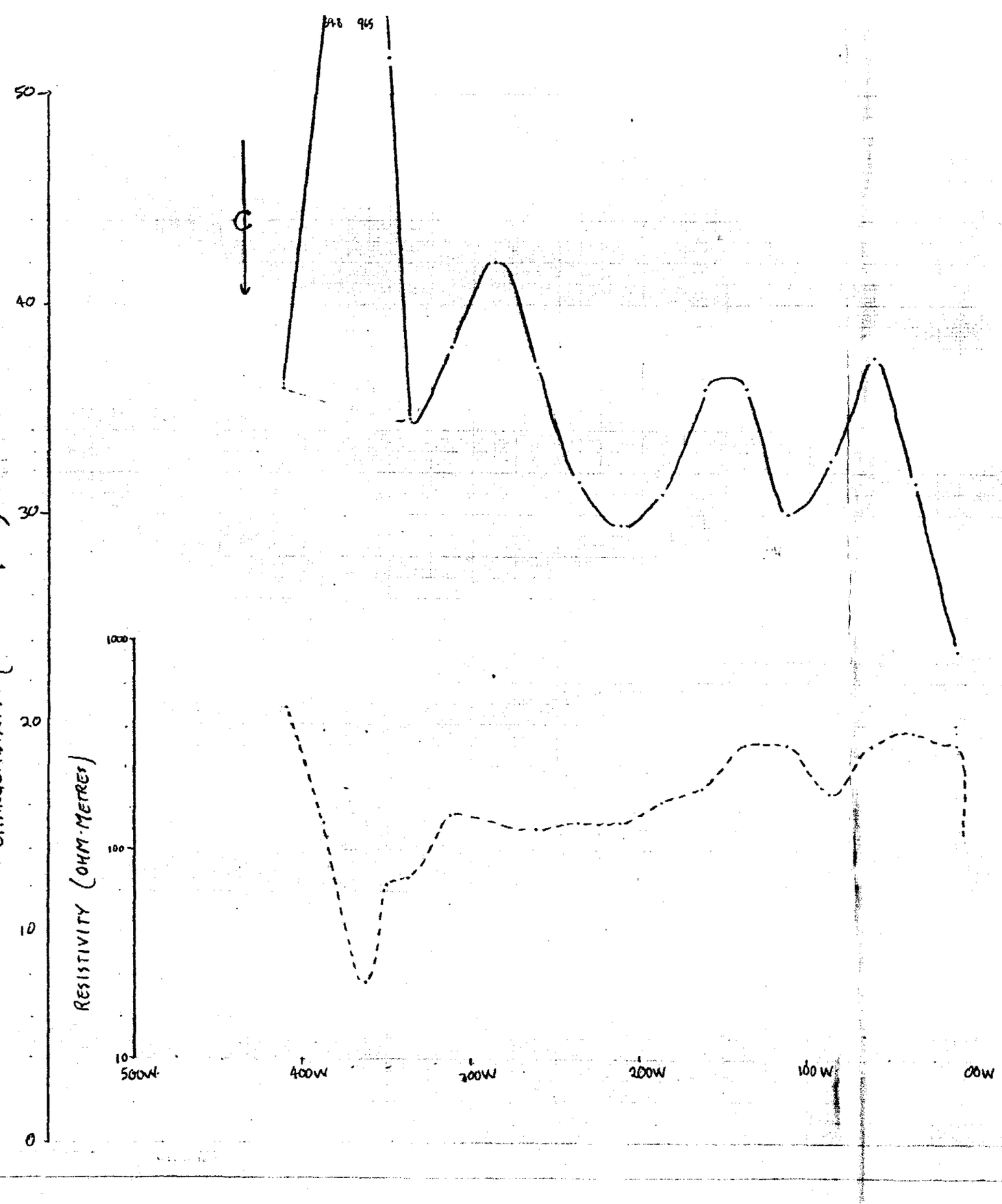

077

317078

LINE 1100N

JOB Nº : TAS-037

AREA : KAPI

DATE : 77-02-13

EIP TIME DOMAIN(2)

C_1-C_2 = 2800m

P_1-P_2 = 25m

5 cm

CHARGEABILITY IN MILLIVOLTS/VOLT

RESISTIVITY IN OHM METRES

M3

M3

R

R

500W 400W 300W 200W 100W 00

076

317079

LINE 1300N.

JOB No-TAS-037

DATE ~ 13-2-77

AREA ~ KRPI

EIP TIME DOMAIN ~2SEC

C_1C_2 = 2800m

P_1P_2 = 25 & 50m.

5 cm

CHARGEABILITY in milliseconds per volt

RESISTIVITY in ohm metres

50
45
40
35
30
25
20
1000
100
10

560 667

1

CREEK

CREEK

M_3 o—o 25m dipole
x—x 50m dipole

R .—. 25m dipole
Δ—. 50m dipole

500W 300W 100W 0.

075

317080

LINE 1500N

JOB NO ~ TAS-037

DATE ~ 11-2-77

AREA ~ KAPI

FIP TIME DOMAIN 2 SEL

C_1C_2 = 2800m

P_1P_2 = 25m

x = 200m.

—x— — — P_1-P_2 = 50m

— o — o — P_1-P_2 = 25m

5 cm

CHARGEABILITY in milliVolts per volt

RESISTIVITY in OHM METERS

TAUNUS

OLD WORKINGS

M_3

R.

50

45

40

35

30

25

20

1000

100

10

10

600W

400W

200W

0

074

317081

LINE 1700N

JOB No ~ TAS-037

DATE ~ 12-2-77

AREA ~ KAPI

EIP TIME DOMAIN ~ 2SEC

C_1C_2 = 2800m

P_1P_2 = 25 or 50m

5 cm

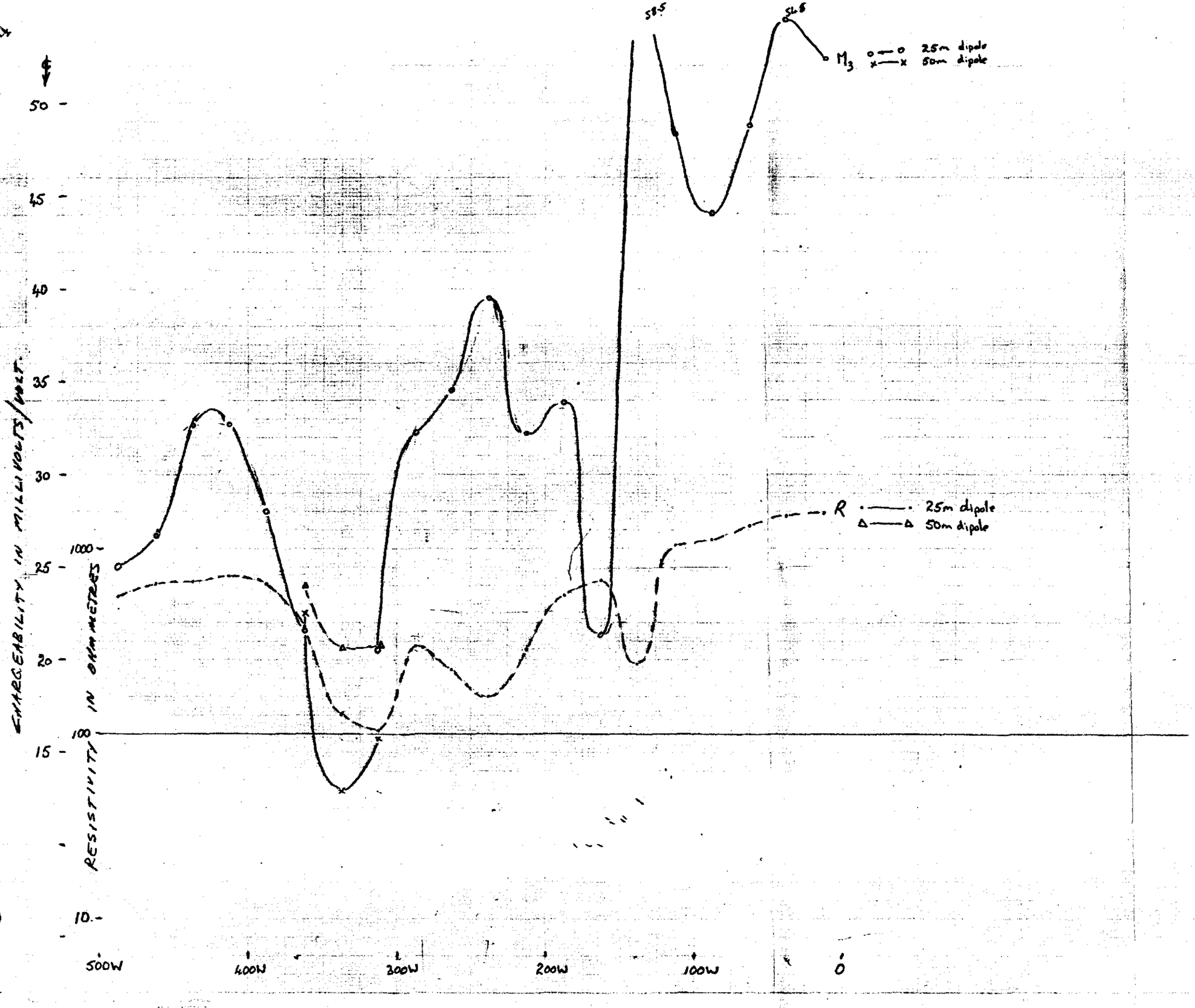

073

317082

LINE 1900N

JOB NO: TAS-037

DATE : 77-02-12

AREA : KAPI

EIP TIME DOMAIN(2S)

$C_1 - C_2 = 2800m$

$P_1 - P_2 = 25m + 50m$

—x—x— $P_1 P_2 = 50m$

—•—•— $P_1 - P_2 = 25m$

5 cm

CHARGEABILITY IN MILLIVOLTS/VOLT

RESISTIVITY IN OHM-METRES

OLD WORKINGS

FAULT

OLD WORKINGS

400W

300W

200W

100W

00

50 45 40 35 30 25 20 15 10 5 0

1000 600 500 400 300 200 100 60 50 40 30 20 10

317083

072

LINE 1900N

JOB No. : TAS 037

AREA : KAPI

DATE : 15/2/77

EIP TIME DOMAIN (2 sec)

C_1C_2 = 2000ms

P_1P_2 = 25m

5 cm

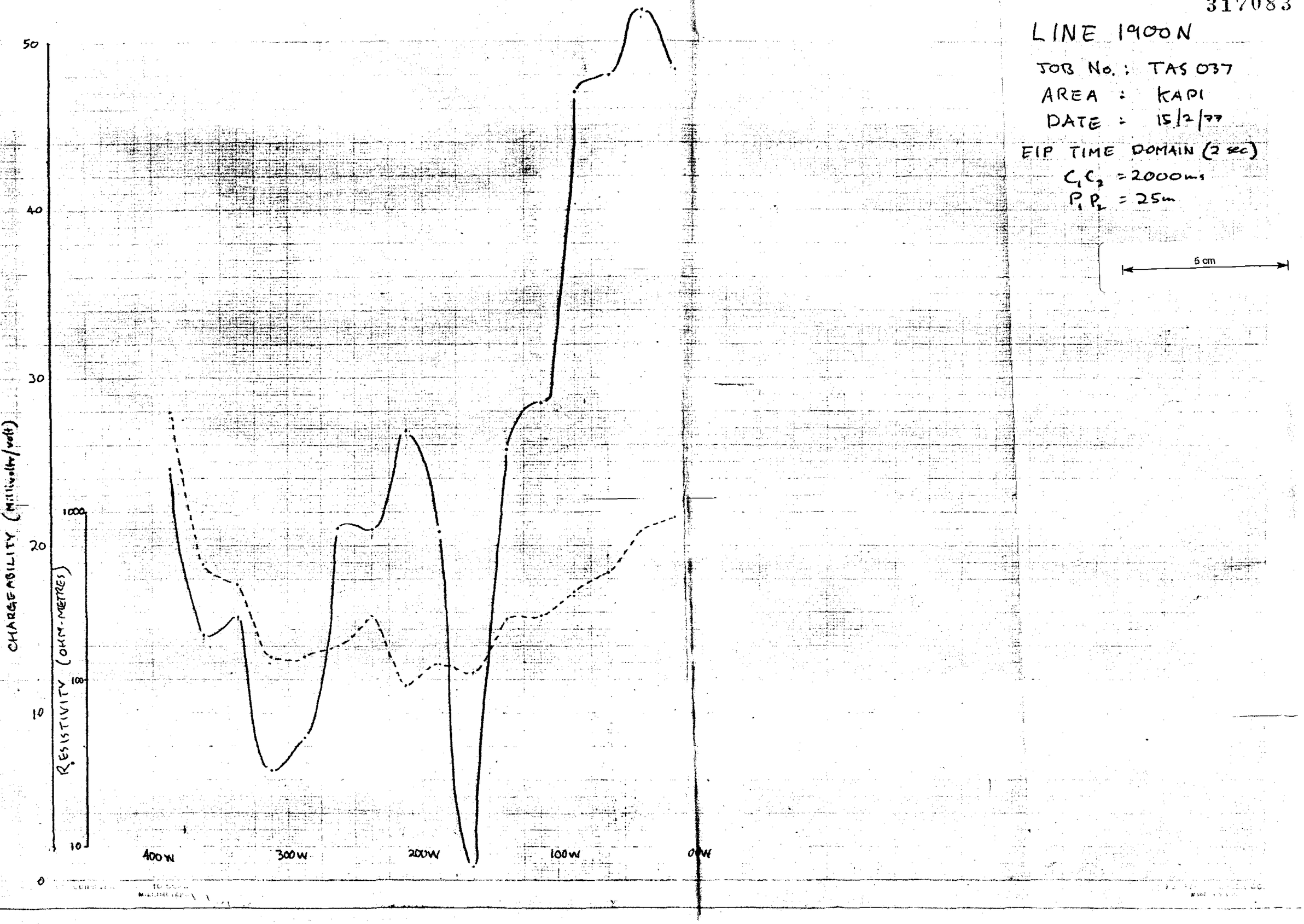

071

LINE 2100N 317084

JOB NO: TAS-037

DATE: 77-02-07

AREA: KAPI

E/P TIMEDOMAIN(2L)

C_1-C_2 = 1200m

P_1-P_2 = 25m

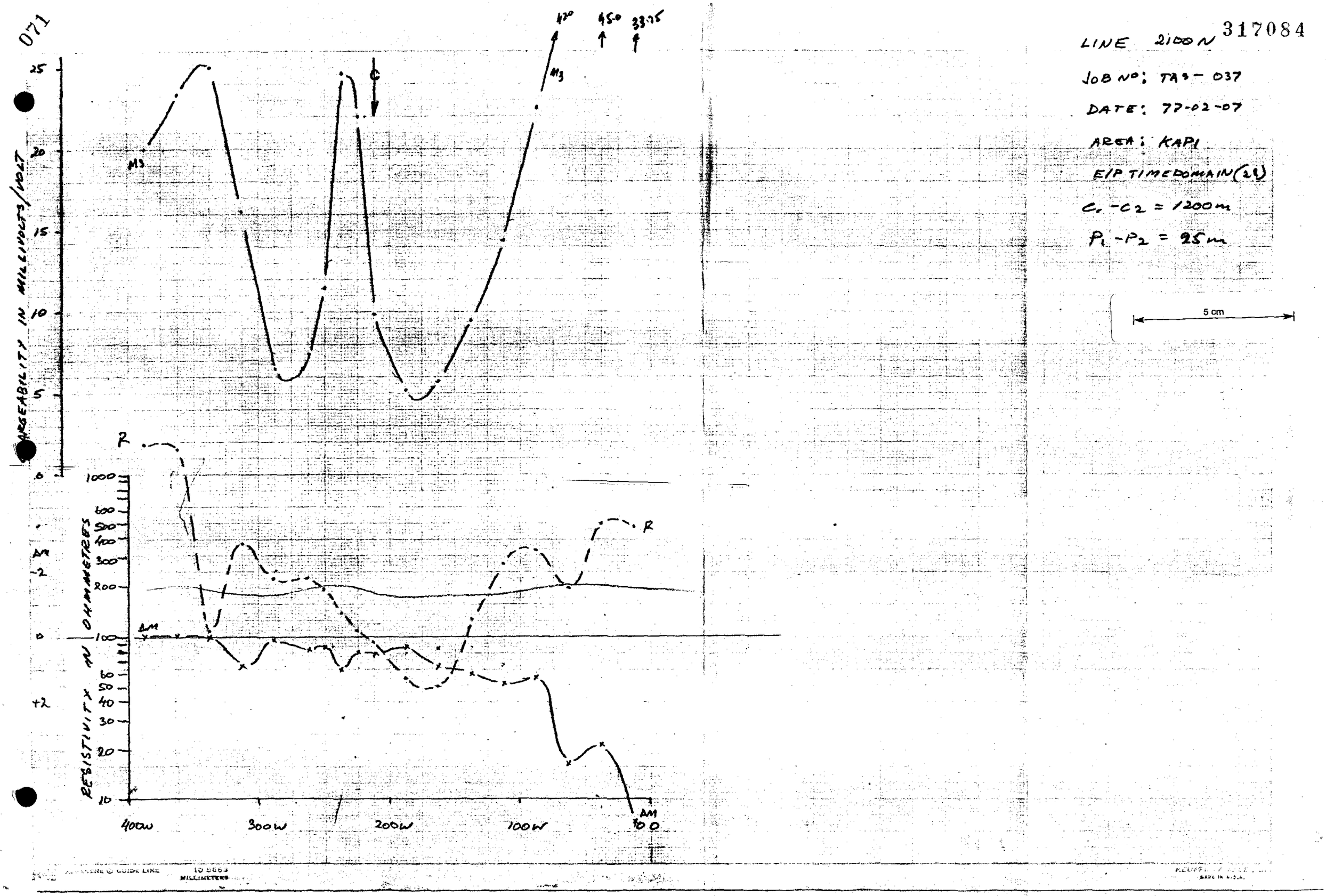

5 cm

070

317085

LINE 2100N

JOB No.: TAS 037
AREA : KAPI
DATE : 15/2/77
E.I.P. TIME DOMAIN (2 sec)
C_1C_2 = 2000ms
P_1P_2 = 25ms.

5 cm

CHARGEABILITY (MILLIVOLTS/VOLT)

50
40
30
20
10

RESITIVITY (OHM-METRES)

1000
100
10

VERY NOISY

700W
300W
200W
100W
0S W.

069

317086

LINE 2300N

JOB NO: TAS-037

DATE: 77-02-06

AREA: KAPI

E.I.P. TIMEDOMAIN (25)

$C_1 - C_2$ = 1200m

$P - P_2$ = 25m

5 cm

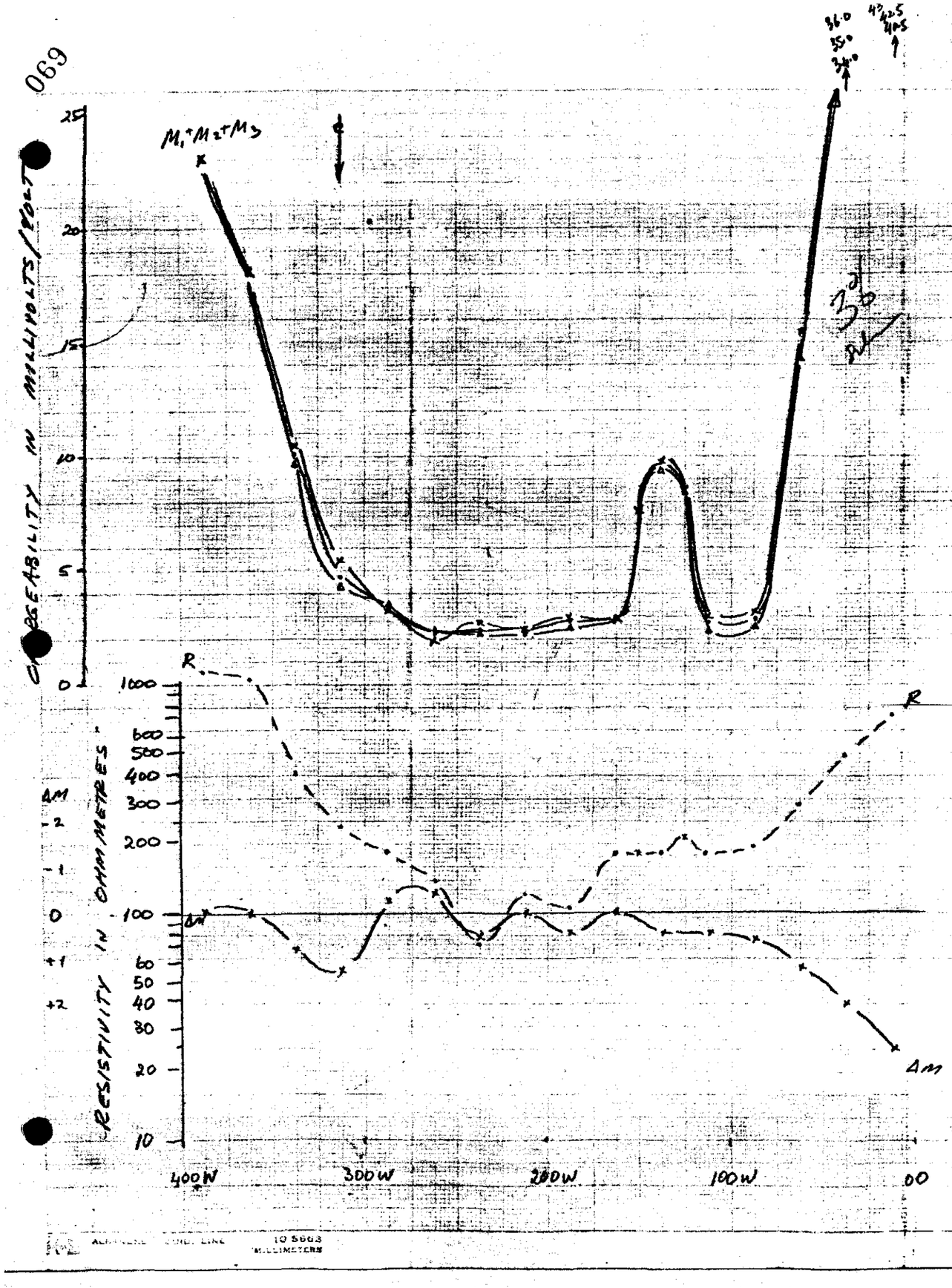

068

317087

LINE 2500N.

JOB NO ~ TAS - 037

DATE ~ 6-2-77

AREA ~ KAPI

EIP TIME DOMAIN 2SEC

C_1C_2 = 1200m.

P_1P_2 = 25m.

5 cm

CHARGEABILITY IN MILLISECS/SEC

M

20

15

10

5

R.

1000

100

10

P_a

M_3

ΔM

-2

0

+2

ΔM IN MILLIMETRES

RESISTIVITY

ΔM

P_{ac}

600W

400W

200W

0

067

317088

2700N.

JOB NO ~ TAS-037

DATE ~ 8-2-77

AREA ~ KAPI

EIP TIME DOMAIN 2SEC

C_1C_2 = 1200m

P_1P_2 = 25m.

5 cm

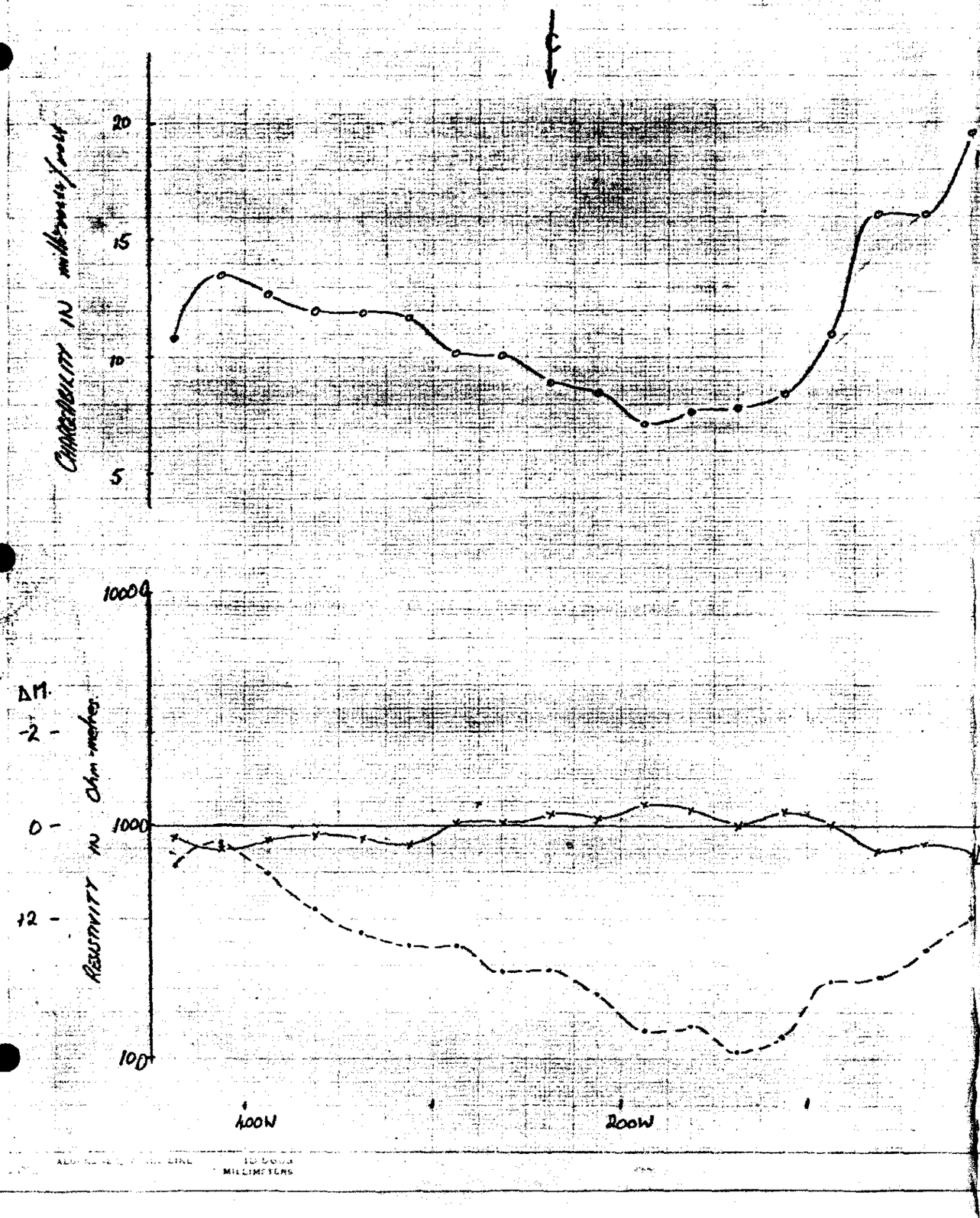

066

317089

LINE 2900N

JOB Nº : TAS - 037

DATE : 77-02-07

AREA : KAPI

EIP TIMEDOMAIN(21)

$C_1 - C_2 = 1200m$

$P_1 - P_2 = 25m$

5 cm

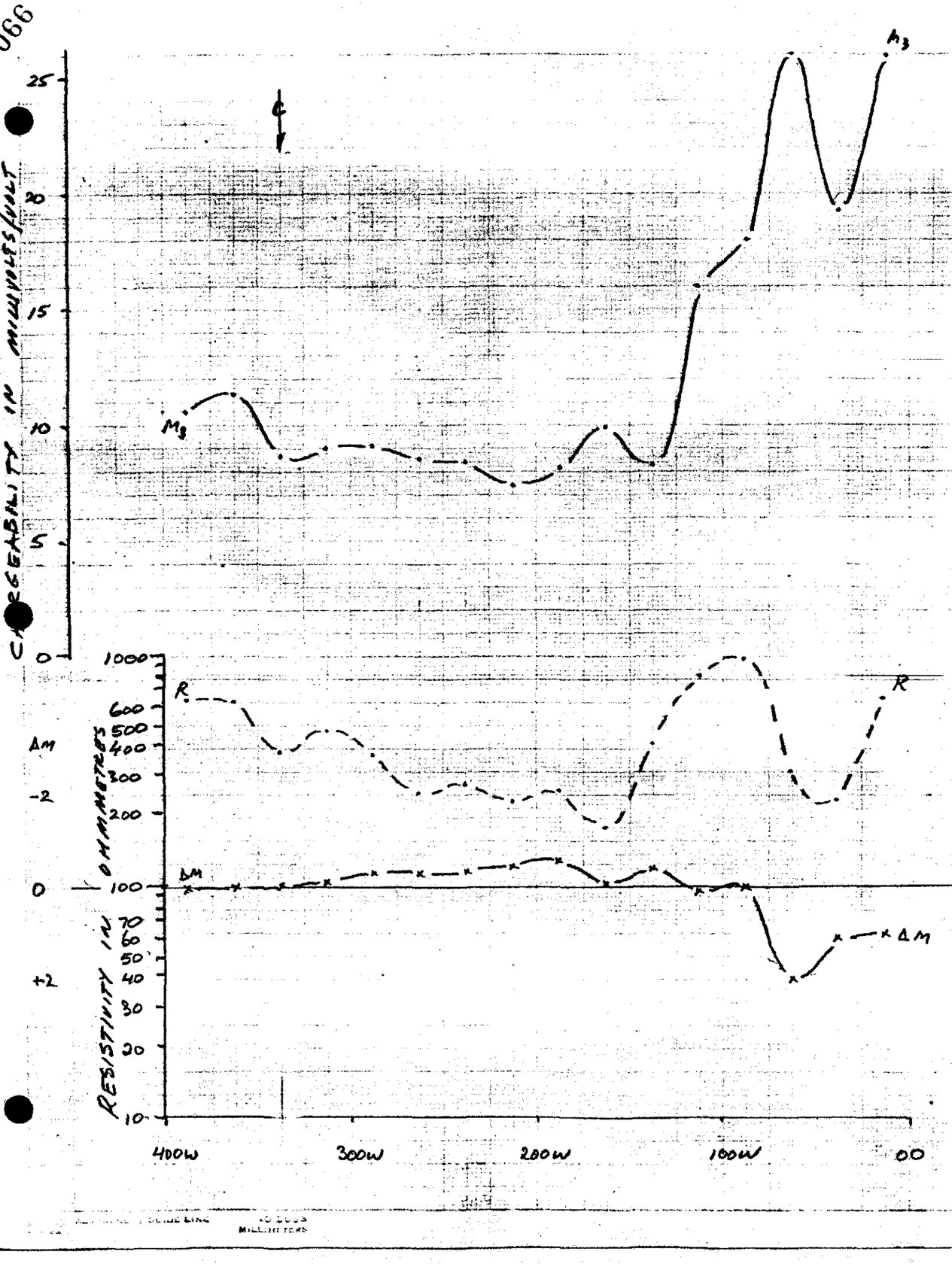

065

317090

LINE 15900 N.

JOB No ~ TAS-037

DATE ~ 9-2-77

AREA ~ KAPI.

EIP TIME DOMAIN ~ 2SEC

C_1C_2 = 900m.

P_1P_2 = 25m.

5 cm

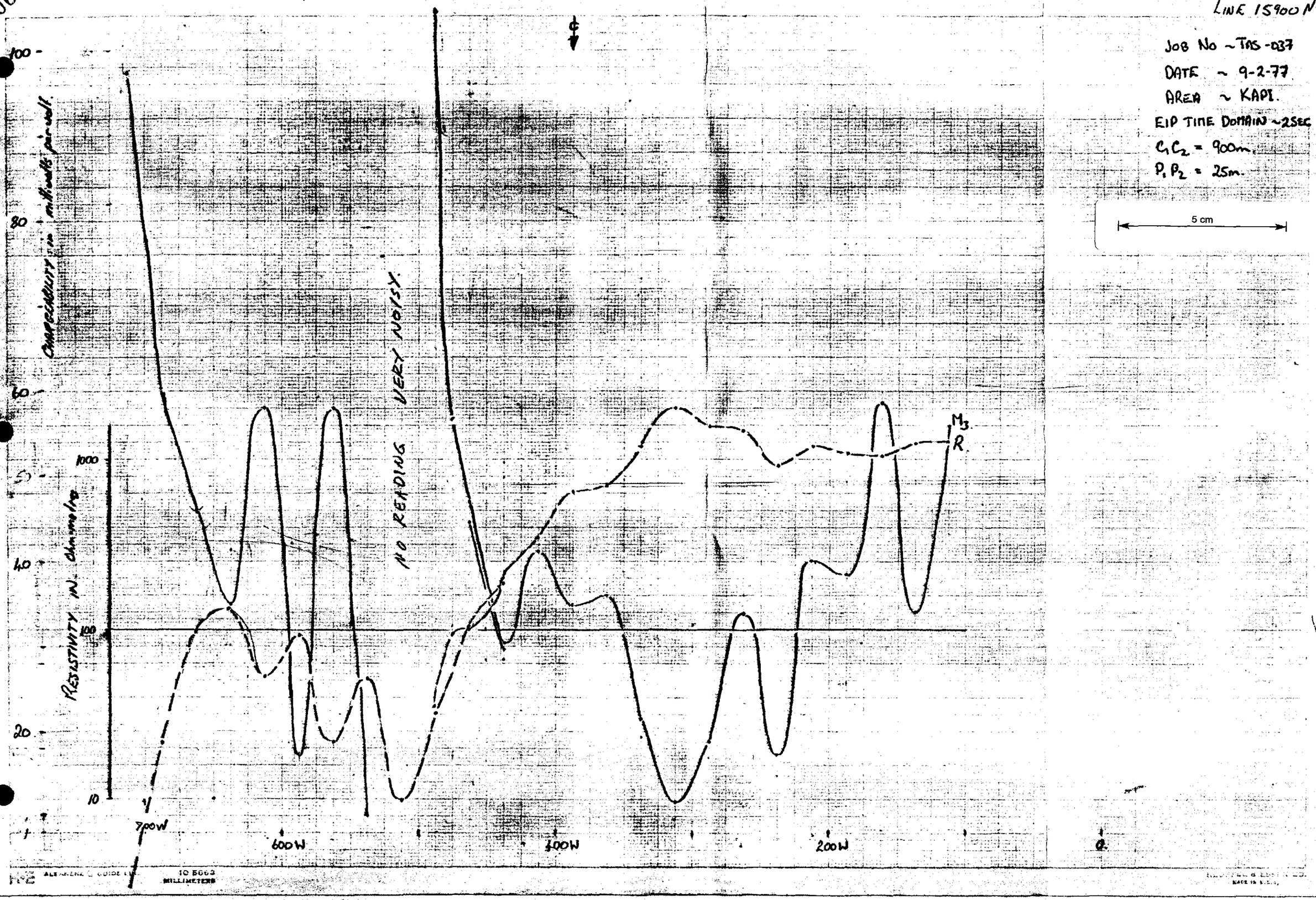

10 5063
MILLIMETERS